Doppelt, S.H., Hill, S.C., Mankin, H.J., Murray, G.J., Parker, R.I., Argoff, C.E., 1991. Replacement therapy for inherited enzyme deficiency—Macrophage-targeted glucocerebrosidase for Gaucher's disease. N. Engl. J. Med. 324, 1464–1470.

Baum, H., Dodgson, K.S., Spencer, B., 1959. The assay of arylsulfatase A and B in human urine. Clin. Chim. 453–455.

Ben-Hur, T., Einstein, O., Mizrachi-Kol, R., Ben-Menachem, O., Reinhartz, E., Karussis, D., Abramsky, O., 2003. Transplanted multipotential neural precursor cells migrate into the inflamed white matter in response to experimental autoimmune encephalomyelitis. Glia 41, 73–80.

Bjorklund, A., Lindvall, O., 2000. Cell replacement therapies for central nervous system disorders. Nat. Neurosci. 3, 537–544.

Bosch, A., Perret, E., Desmaris, N., Heard, J.M., 2000. Long-term and significant correction of brain lesions in adult mucopolysaccharidosis type VII mice using recombinant AAV vectors. Mol. Ther. 1, 63–70.

Bottenstein, J.E., Sato, G.H., 1979. Growth of a rat neuroblastoma cell line in serum-free supplemented medium. Proc. Natl. Acad. Sci. U. S. A. 76, 514–517.

Brady, R.O., Schiffmann, R., 2000. Clinical features of and recent advances in therapy for Fabry disease. J. Amer. Med. Assoc. 284, 2771–2775.

Brazelton, T.R., Rossi, F.M., Keshet, G.I., Blau, H.M., 2000. From marrow to brain: expression of neuronal phenotypes in adult mice. Science 290, 1775–1779.

Buchet, D., Serguera, C., Zennou, V., Charneau, P., Mallet, J., 2002. Long-term expression of beta-glucuronidase by genetically modified human neural progenitor cells grafted into the mouse central nervous system. Mol. Cell. Neurosci. 19, 389–401.

Consiglio, A., Quattrini, A., Martino, S., Bensadoun, J.C., Dolcetta, D., Trojani, A., Benaglia, G., Marchesini, S., Cestari, V., Oliverio, A., Bordignon, B.C., Naldini, L., 2001. In vivo gene therapy of metachromatic leukodystrophy by lentiviral vectors: correction of neuropathology and protection against learning impairments in affected mice. Nat. Med. 7, 310–316.

Dierks, T., Schmidt, B., Borissenko, L.V., Peng, J., Presser, A., Mariappan, M., von Figura, K., 2003. Multiple sulfatase deficiency is caused by mutations in gene encoding the human Cα-formylglycine generating enzyme. Cell 113, 435–444.

Eng, C.M., Banikazemi, M., Gordon, R.E., Goldman, M., Phelps, R., Kim, L., Gass, A., Winston, J., Dikman, S., Fallon, J.T., Brodie, S., Stacy, C.B., Mehta, D., Parsons, R., Norton, K., O'Callaghan, M., Desnick, R.J., 2001. A phase 1/2 clinical trial of enzyme replacement in Fabry disease: pharmacokinetic, substrate clearance, and safety studies. Am. J. Hum. Genet. 68, 711–722.

Falk, A., Holmstrom, N., Carlen, M., Cassidy, R., Lundberg, C., Frisen, J., 2002. Gene delivery to adult neural stem cells. Exp. Cell Res. 279, 34–39.

Gieselmann, V., 2003. Metachromatic leukodystrophy: recent research developments. J. Child Neurol. 18, 591–594.

Gieselmann, V., Matzner, U., Hess, B., Lullmann-Rauch, R., Coenen, R., Hartmann, D., D'Hooge, R., Deyn, P.D., Nagels, G., 1998. Metachromatic leukodystrophy: molecular genetics and an animal model. J. Inherited Metab. Dis. 21, 564–574.

Hess, B., Saftig, P., Hartmann, D., Coenen, R., Lullmann-Rauch, R., Goebel, H.H., Evers, M., von Figura, K., D'Hooge, R., Nagels, G., De Deyn, P., Peters, C., Gieselmann, V., 1996. Phenotype of arylsulfatase A-deficient mice: relationship to human metachromatic leukodystrophy. Proc. Natl. Acad. Sci. U. S. A. 93, 14821–14826.

Hughes, S.M., Moussavi-Harami, F., Sauter, S.L., Davidson, B.L., 2002. Viral-mediated gene transfer to mouse primary neural progenitor cells. Mol. Ther. 5, 16–24.

Igarashi, T., Miyake, K., Kato, K., Watanabe, A., Ishizaki, M., Ohara, K., Shimada, T., 2003. Lentivirus-mediated expression of angiostatin efficiently inhibits neovascularization in a murine proliferative retinopathy model. Gene Ther. 10, 219–226.

Kakkis, E.D., Muenzer, J., Tiller, G.E., Waber, L., Belmont, J., Passage, M., Izykowski, B., Phillips, J., Doroshow, R., Walot, I., Hoft, R., Neufeld, E.F., 2001. Enzyme-replacement therapy in mucopolysaccharidosis I. N. Engl. J. Med. 344, 182–188.

Karlsson, S., 1991. Treatment of genetic defects in hematopoietic cell function by gene transfer. Blood 78, 2481–2492.

Kornfeld, S., 1992. Structure and function of the mannose 6-phosphate/insulinlike growth factor II receptors. Annu. Rev. Biochem. 61, 307–330.

Krivit, W., Shapiro, E., Kennedy, W., Lipton, M., Lockman, L., Smith, S., Summers, C.G., Wenger, D.A., Tsai, M.Y., N.Ramsay, K.C., Kersey, J.H., Yao, J.K., Kaye, E., 1990. Treatment of late infantile metachromatic leukodystrophy by bone marrow transplantation. N. Engl. J. Med. 322, 28–32.

Matzner, U., Habetha, M., Gieselmann, V., 2000. Retrovirally expressed human arylsulfatase A corrects the metabolic defect of arylsulfatase A-deficient mouse cells. Gene Ther. 7, 805–812.

Matzner, U., Hartmann, D., Lullmann-Rauch, R., Coenen, R., Rothert, F., Mansson, J.E., Fredman, P., D'Hooge, R., De Deyn, P.P., Gieselmann, V., 2002. Bone marrow stem cell-based gene transfer in a mouse model for metachromatic leukodystrophy: effects on visceral and nervous system disease manifestations. Gene Ther. 9, 53–63.

Mezey, E., Chandross, K.J., Harta, G., Maki, R.A., McKercher, S.R., 2000. Turning blood into brain: cells bearing neuronal antigens generated in vivo from bone marrow. Science 290, 1779–1782.

Migita, M., Hamada, H., Fujimura, J., Watanabe, A., Shimada, T., Fukunaga, Y., 2003. Glucocerebrosidase level in the cerebrospinal fluid during enzyme replacement therapy—unsuccessful treatment of the neurological abnormality in type 2 Gaucher disease. Eur. J. Pediatr. 62, 524–525.

Ohashi, T., Watabe, K., Uehara, K., Sly, W.S., Vogler, C., Eto, Y., 1997. Adenovirus-mediated gene transfer and expression of human beta-glucuronidase gene in the liver, spleen, and central nervous system in mucopolysaccharidosis type VII mice. Proc. Natl. Acad. Sci. U. S. A. 94, 1287–1292.

Okabe, M., Ikawa, M., Kominami, K., Nakanishi, T., Nishimune, Y., 1997. Green mice as a source of ubiquitous green cells. FEBS Lett. 407, 313–319.

Ostenfeld, T., Tai, Y.T., Martin, P., Degon, N., Aebischer, P., Svendesen, C.N., 2002. Neurospheres modified to produce glial cell line-derived neurotrophic factor increase the survival of transplanted dopamine neurons. J. Neurosci. Res. 69, 956–965.

Piccini, P., Brooks, D.J., Bjorklund, A., Gunn, R.N., Grasby, P.M., Rimoldi, O., Brundin, P., Hagell, P., Rehncrona, S., Widner, H., Lindvall, O., 1999. Dopamine release from nigral transplants visualized in vivo in a Parkinson's patient. Nat. Neurosci. 2, 1137–1140.

Pluchino, S., Quattrini, A., Brambilla, E., Gritti, A., Salani, G., Dina, G., Galli, R., DelCarro, U., Amadio, S., Bergami, A., Furlan, R., Comi, G., Vescovi, A.L., Martino, G., 2003. Injection of adult neurospheres induces recovery in a chronic model of multiple sclerosis. Nature 422, 688–694.

Reynolds, B.A., Weiss, S., 1992. Generation of neurons and astrocytes from isolated cells of the adult mammalian central nervous system. Science 255, 1707–1710.

Reynolds, B.A., Tetzlaff, W., Weiss, S., 1992. A multipotent EGF-responsive striatal embryonic progenitor cell produces neurons and astrocytes. J. Neurosci. 12, 4565–4574.

Schiffmann, R., Kopp, J.B., Austin III, H.A., Sabnis, S., Moore, D.F., Weibel, T., Balow, J.E., Brady, R.O., 2001. Enzyme replacement therapy in Fabry disease: a randomized controlled trial. J. Amer. Med. Assoc. 285, 2743–2749.

Schumm, M.A., Castellanos, D.A., Frydel, B.R., Segan, J., 2004. Improved neural progenitor cell survival when congrafted with chromaffin cells in rat striatum. Exp. Neurol. 185, 133–142.

Shapiro, E.G., Lockman, L.A., Balthazor, M., Krivit, W., 1995. Neuropsychological outcomes of several storage diseases with

and without bone marrow transplantation. J. Inherited Metab. Dis. 18, 413–429.
Stein, C., Gieselmann, V., 1989. Cloning and expression of human arylsulfatase A. J. Biol. Chem. 264, 1252–1259.
Suzuki, A., Obi, K., Urabe, T., Hayakawa, H., Yamada, M., Kaneko, S., Onodera, M., Mizuno, Y., Mochizuki, H., 2002. Feasibility of ex vivo gene therapy for neurological disorders using the new retroviral vector GCDNsap packaged in the vesicular stomatitis virus G protein. J. Neurochem. 82, 953–960.
Von Figura, K., Gieselmann, V., Jaeken, J., 2001. Metachromatic leukodystrophy. In: Scriver, C.R., Beaudet, A.L., Sly, W.S., Valle, D. (Eds.), The Metabolic and Molecular Bases of Inherited Disease, pp. 3695–3724.
Wei, J.F., Wei, F.S., Samulski, R.J., Barranger, J.A., 1994. Expression of the human glucocerebrosidase and arylsulfatase A genes in murine and patient primary fibroblasts transduced by an adeno-associated virus vector. Gene Ther. 1, 261–268.
Yandava, B.D., Billinghurst, L.L., Snyder, E.Y., 1999. "Global" cell replacement is feasible via neural stem cell transplantation: evidence from the dysmyelinated shiverer mouse brain. Proc. Natl. Acad. Sci. U. S. A. 96, 7029–7034.
Zirzow, G.C., Sanchez, O.A., Murray, G.J., Brady, R.O., Oldfield, E.H., 1999. Delivery, distribution, and neuronal uptake of exogenous mannose-terminal glucocerebrosidase in the intact rat brain. Neurochem. Res. 24, 301–305.

ELSEVIER

Brain & Development 28 (2006) 420–425

BRAIN & DEVELOPMENT
Official Journal of the Japanese Society of Child Neurology

www.elsevier.com/locate/braindev

Original article

Adenoviral mediated MyoD gene transfer into fibroblasts: Myogenic disease diagnosis

Isao Fujii [a,b,*], Makoto Matsukura [a,b], Makoto Ikezawa [b], Satoru Suzuki [c], Takashi Shimada [c], Teruhisa Miike [b]

[a] *Division of Clinical Pharmacy, Laboratory of Clinical Pharmacology and Therapeutics, Department of Pharmaceutical Sciences, Faculty of Pharmaceutical Sciences, Sojo University, 4-22-1 Ikeda, Kumamoto-city, Kumamoto 860-0082, Japan*
[b] *Department of Child Development, School of Medicine, Kumamoto University, Kumamoto, Japan*
[c] *Division of Gene Therapy Research, Department of Biochemistry and Molecular Biology, Center for Advanced Medical Technology, Nippon Medical School, Tokyo, Japan*

Received 13 September 2004; received in revised form 14 November 2005; accepted 26 December 2005

Abstract

MyoD, a master regulatory gene for myogenesis, converts mesoderm derived cells to the skeletal muscle phenotype MyoD gene transfer into skin fibroblasts has been attempted in an effort to diagnose genetic muscle diseases. Although the gene transduction efficiency of adenoviral gene delivery systems is higher than that of various other systems, the rate of myo-conversion is insignificant. Since high adenovirus doses are cytotoxic and exogenous MyoD expression is insufficient for skin fibroblasts to re-differentiate into muscle cells, we constructed the novel adeno-MyoD vector, Ad.CAGMyoD using the recombinant CAG promoter. Even at a lower multiplicities of infection most skin fibroblasts infected with Ad.CAGMyoD could convert into myotubes without vector-induced cytotoxicity. The converted cells expressed muscle-specific desmin and full-length dystrophin, both of which were detected by Western blotting. Genetic and immunohistochemical analyses using skin fibroblasts and our vector system are reliable and useful for the clinical diagnosis of genetic muscle diseases.

Keywords: MyoD; Myogenesis; Muscular disease; Genetic diagnosis

1. Introduction

Muscle biopsy is a standard method of evaluating histopathological, histochemical, and immunohistochemical changes associated with genetic muscle diseases. In addition, the genetic background and/or the gene expression profile can be determined from DNA and/or RNA that is extracted from biopsy specimens [1]. Muscle biopsy can be performed in adults under local anesthesia, which is not risky even when patients have muscular diseases. However, general anesthesia is necessary for muscle biopsies in young pediatric patients and this poses a significant risk of malignant hyperthermia when children have muscular diseases [2]. In addition to the risks, histological changes in muscle tissue are sometimes progressive and biopsies can therefore be unsuitable as diagnostic markers.

Multiplex PCR using DNA and/or RNA extracted from blood can overcome the shortcomings described above in patients with Duchenne and Becker muscular dystrophies (DMD and BMD) [3]. However, only 50–60% of clinically suspected muscular dystrophy patients have been conclusively diagnosed using this method. Rather, the forced myogenesis of non-muscle cells (e.g. skin fibroblasts and amniotic fluid cells) with viral vector-mediated MyoD cDNA transduction is useful [4–10]. MyoD is one of the genes that regulate mammalian skeletal muscle development, and therefore, myogenesis mediated by MyoD theoretically allows the investigation of muscle-specific gene expression and proteins in non-muscle cells [11–14]. However, the efficiency of myo-conversion is not consistently high enough for practical diagnostic studies [7].

* Corresponding author. Address: Division of Clinical Pharmacy, Laboratory of Clinical Pharmacology and Therapeutics, Department of Pharmaceutical Sciences, Faculty of Pharmaceutical Sciences, Sojo University, 4-22-1 Ikeda, Kumamoto-city, Kumamoto 860-0082, Japan. Tel.: +81 96 326 4085; fax: +81 96 326 5048.
E-mail address: isa-f@ph.sojo-u.ac.jp (I. Fujii).

0387-7604/$ - see front matter © 2006 Elsevier B.V. All rights reserved.
doi:10.1016/j.braindev.2005.12.007

To address this issue, we constructed a novel adenoviral expression vector, Ad.CAGMyoD, which contains MyoD cDNA under the control of the powerful recombinant CAG promoter [15]. Here, we show that the Ad.CAGMyoD vector will be a useful tool for the genetic, histochemical and immunohistochemical diagnoses of muscle diseases.

2. Materials and methods

2.1. Cells

We established skin fibroblasts from a 2-year-old patient with Duchenne muscular dystrophy (DMD) and performed a simultaneous muscle biopsy as follows. In addition, we acquired control skin fibroblasts from another patient from whom a skin biopsy confirmed the diagnosis of an undetermined non-muscular metabolic disease. We obtained the written informed consent of the parents confirming that both children could participate in the study, which was approved by our institutional Ethics Committee. Skin fragments were finely minced with scissors in RPMI medium, plated into a 60 mm dish and incubated Dulbecco's modified Eagle's medium (DMEM) supplemented with 10% fetal calf serum (FCS). After 4–5 days, fibroblasts began to proliferate from the fragment margin and created monolayer. The outgrowing cells were morphologically consistent with fibroblasts by their characteristic spindle-shaped appearance. All experiments were carried out with cells derived from up to four passages.

2.2. Adenoviral vector construction

We generated recombinant adenoviral vectors using the Saito method as reported [16]. Briefly, we excised the MyoD expression unit containing murine MyoD cDNA under the control of the CAG promoter from pCAGGS-MyoD. Murine MyoD cDNA was a gift from Dr Y. Nabeshima (National Institute of Neurology, Tokyo). The CAGGS-MyoD unit was inserted into the SwaI site of the pAdexlw cosmid that contained the genome of adenovirus type 5 without the E1 and E3 regions. The cosmid was co-transfected with the EcoT221-digested adenovirus DNA-terminal protein complex into 293 cells by calcium phosphate co-precipitation. The recombinant adenovirus vector, Ad.CAGMyoD, was isolated, amplified and purified by double CsCl gradient centrifugation [17]. The titer of Ad.CAGMyoD determined by the end-point cytopathic assay was 1×10^9 PFU/ml. The control vector, Ad.CAGEGFP, which contained the EGFP cDNA under the control of the CAG promoter, was prepared in the same manner as Ad.CAGMyoD and the titer was 1×10^9 PFU/ml. The final preparations were stored at −80 °C.

2.3. Adenoviral transduction

Primary skin fibroblasts seeded at a density of 1×10^6 cells per well of six well collagen coated culture plates were infected with Ad.CAGMyoD at several multiplicities of infection (moi) in FCS free DMEM for 1 h. The cells were rinsed twice with phosphate buffered saline (PBS), and cultured in DMEM containing 10% FCS for 2 days, followed by DMEM containing 2% FCS for myogenic induction.

2.4. Toxicity assay

The vector toxicity towards the cells was detected by the MTT assay (CellTiter 96® AQueous Non-Radioactive Cell Proliferation Assay, Promega) on day 7 after infection.

2.5. Western blotting

Primary fibroblasts infected with Ad.CAGMyoD were rinsed twice with PBS, scraped from the plates, and then sedimented by centrifugation. Cell pellets were re-suspended in 50 μl of sample buffer (40 mM Tris, pH 8.0, 240 mM glycine, 8 mM EDTA, 10% SDS, 0.03% bromophenol blue, 40% glycerol, 100 mM DTT, 2 μg/ml aprotinin, 0.5 μg/ml leupeptin hemisulphate, 2 mM PMSF), homogenized with a 27 G needle, heated to 95 °C for 10 min, and then centrifuged. Samples were loaded on a 4–15% SDS-PAGE gradient gel (in 250 mM Tris, 192 mM glycine, 0.1% SDS) and then transferred to Hybond™ ECLTM nitrocellulose membranes (in 200 mM Tris, 192 mM glycine, 0.1% SDS, 20% methyl alcohol). To detect MyoD, desmin or dystrophin, the nitrocellulose membranes were incubated for 90 min at room temperature with antibodies to NCL-MyoD1 (1:20, Novocastra), DE-U-10 (1:150, Sigma), or NCL-Dys2 (1:100, Novocastra), respectively. NCL-MyoD1 is a mouse monoclonal antibody that recognizes an epitope near the C-terminus of MyoD1 protein. DE-U-10 is a mouse monoclonal anti-desmin antibody. NCL-Dys2 is a mouse monoclonal antibody that recognizes the C-terminus between amino acids 3669 and 3685 of human dystrophin. The internal control for loaded samples was the same membrane incubated with an anti β-catenin mouse monoclonal antibody (1:2000, Transduction Laboratories). Bound antibodies were visualized by subsequent chemiluminescent reaction with a horseradish peroxidase conjugated goat antibody to mouse IgG (1:20,000, ICN) in the ECL system (Amersham).

2.6. Immunocytochemistry

After various periods of Ad.CAGMyoD infection at an moi of 50, cultured cells were fixed and stained with antibodies to desmin (1:20, DE-U-10) or dystrophin (1:20, NCL-Dys2). Bound antibodies were visualized using a VECTASTAIN

ABC Goat IgG Kit (Vector Laboratories, Inc.) and a secondary biotin conjugated goat antibody to mouse IgG.

3. Results and discussion

3.1. MyoD protein expression

We evaluated the ability of Ad.CAGMyoD to express MyoD protein in human primary fibroblasts. Cells were infected with Ad.CAGMyoD at an moi of 1, 3, 10, 30, 100 or 300, harvested 2 days later, and then Western blotted. MyoD protein appeared at an moi of 10 and then increased with the dose of Ad.CAGMyoD dependent manner (Fig. 1A). The viability of infected cells, however, decreased at an moi above 100 (Fig. 1B).

3.2. Myogenic conversion induced by MyoD expression

Since MyoD per se is a regulatory gene for myogenesis, molecules in MyoD transduced cells should sequentially change towards myogenesis [18]. Desmin, one of the earliest well-known muscle-specific structural protein during skeletal muscle development [19], were used to examine the pattern of myogenesis. By immunocytochemical method with anti-desmin antibody, we found that transduction of Ad.CAGMyoD at an moi of 3, 10, and 30 converted the fibroblast cells to myotubes 2–5, 15–20, and, 50–65%, respectively. Thus, conversion efficiency increased linearly by increasing the moi and reached a plateau at an moi of 100. However, at this relatively high moi, cytotoxicity was apparent and approximately a half of the plated cells was dead after 6 days in culture (data not shown). On the other hand, over 80% of Ad.CAGMyoD transduced cells were desmin positive with at an moi of 50 without cytotoxicity (Fig. 2). These results indicated that the optimal moi of Ad.CAGMyoD transduction was 50, so we used this level of infection for subsequent studies of primary human skin fibroblasts.

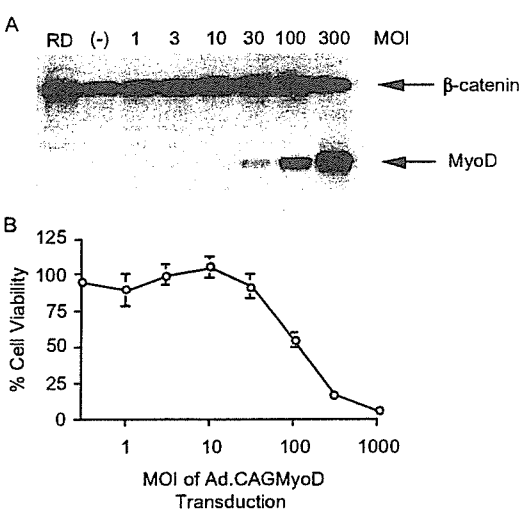

Fig. 1. Expression of MyoD protein in human fibroblast culture after Ad.CAGMyoD transduction at various moi (A). Western blotting proceeded 2 days after Ad.CAGMyoD transduction. Extracted proteins separated on 4.5–15% polyacrylamide SDS-PAGE gels were immunoblotted with antibodies against MyoD and internal standard β-catenin. Cell viabilities of human fibroblast culture after transduction with Ad.CAGMyoD at various moi (B). Data were obtained 7 days after Ad.CAGMyoD transduction.

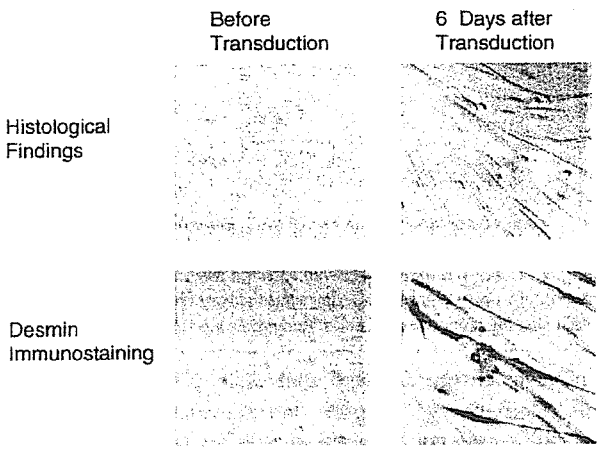

Fig. 2. Histochemical detection of desmin in human fibroblast culture before or after Ad.CAGMyoD transduction. Desmin staining was carried out before or 6 days after Ad.CAGMyoD transduction at moi of 50.

Morphological changes towards myotubes were observed by microscopy from 72 h after infection and these increased over time (data not shown). To understand the molecular mechanism involved in this change, we sought the relationship between the MyoD's effects and desmin expression. Human primary skin fibroblasts transduced with Ad.CAGMyoD at an moi of 50 were harvested after 6, 12, 24, 48, 72 or 120 h. As shown in Fig. 3, MyoD expression in skin fibroblast increases the developmental switch from desmin gene expression after 48 h of Ad.CAGMyoD transduction.

3.3. Application to genetic diagnosis

To examine the applicability of the Ad.CAGMyoD system to the genetic diagnosis of musclular diseases, we use fibroblasts from a patient with DMD as a typical genetic muscle disease and investigated whether DMD fibroblast cells could be converted to myotubes without dystrophin, which is not present in DMD muscle [20]. Fibroblasts obtained from a patient with a non-musclular disease were applied to the control dystrophin positive cells. The Ad.CAGEGFP vector containing the EGFP gene driven by the same CAG promoter was utilized as the control adenoviral vector. The EGFP gene encodes recombinant green fluorescent protein, which does not effect myogenic conversion [21].

Western blot studies showed that full-length dystrophin protein as well as desmin was observed in non-muscular

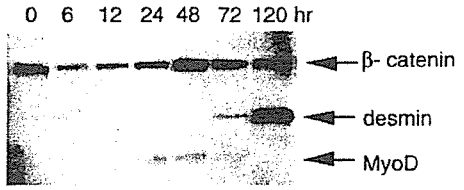

Fig. 3. Time course analysis of MyoD and desmin expression in human fibroblast culture transduced with Ad.CAGMyoD at moi of 50. Western blot analysis showed that MyoD was detected from 24 through 72 h after transduction. Forty-eight hours after transduction, muscle-specific desmin protein was become to express and increased over time.

fibroblasts 14 and 21 days after Ad.CAGMyoD transduction. Conversely, despite the expression of desmin, dystrophin was not detected in Ad.CAGMyoD transduced DMD fibroblasts even on day 21. Desmin was not expressed in samples with Ad.CAGEGFP transduction (Fig. 4A).

Histological analysis clearly revealed immunostained dystrophin in converted myotubes from the patient with the non-muscular disease. In contrast, although Ad.CAGMyoD transduced DMD fibroblasts also started to shift towards myotubes after day 3, dystrophin was not stained eventually in morphologically well-converted DMD myotubes on day 21 (Fig. 4B). No morphological changes were observed in Ad.CAGEGFP transduced fibroblasts from both patients (data not shown).

3.4. Discussion

Because MyoD protein binds to sequences in the enhancers or promoters of other myogenic regulatory genes, such as the Myf5, myogenin, and MRF4 genes, and triggers their expression, MyoD protein is a key muscle-specific transcriptional factor [8,9]. The constitutive muscle-specific gene expression, such as of desmin and dystrophin, follows that of MyoD and other myogenic regulatory genes [22,23].

Previous studies have shown that the recombinant viral vector mediated exogenous MyoD expression in mesoderm cells could cause their conversion to the myogenic phenotype. Weintraub et al. have constructed an amphotropic retroviral vector containing MyoD cDNA driven by the MoMLV long terminal repeat [7]. Probably because of the poor transduction efficiency of the retroviral vector, infected target cells had to be selected in medium containing G418 to obtain MyoD positive cells. Although an active cell cycle is necessary for G418 selection, the MyoD protein per se induces cell cycle arrest through the activation of p21, a Cdk inhibitor [24]. Probably due to this dilemma, cells selected in medium containing G418 were more resistant to G418 and expressed less MyoD. We also found that extremely low levels of MyoD expression were induced using the same retroviral vector system (data not shown).

Adenoviral vectors have often been used to overcome low transduction efficiency despite the transient nature of exogenous gene expression. However, MyoD expression

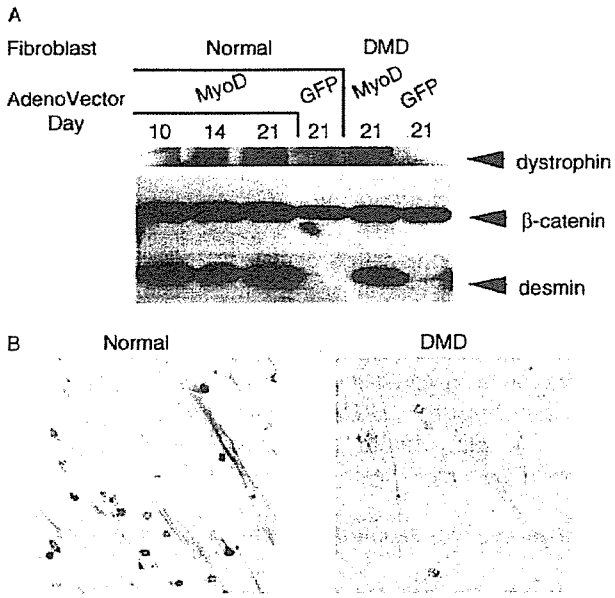

Fig. 4. Time course analysis of dystrophin expression in human fibroblast culture transduced with the recombinant adenoviral vectors at moi of 50 (A). Ad.CAGMyoD transduced fibroblasts from patient with non-musclular disease were cultured for 10, 14 or 21 days. Ad.CAGEGFP transduced fibroblasts from patient with non-musclular disease were cultured for 21 days. Ad.CAGMyoD or Ad.CAGEGFP transduced fibroblasts from DMD patient were also cultured for 21 days. MyoD: Ad.CAGMyoD; EGFP: Ad.CAGEGFP; Normal: non-muscular disease; DMD: Duchenne muscular dystrophy. Histochemical detection of dystrophin in human fibroblast culture 21 days after transduction with Ad.CAGMyoD at moi of 50 (B). Dystrophin staining was carried out in morphologically well-converted myotubes from both the patient with the non-muscular disease and DMD patient.

starts at 18 h after muscle necrosis, reaches the maximum level at 48 h and then decreases, indicating that transient MyoD expression is sufficient for myogenesis [25]. Murry et al. constructed a recombinant adenoviral vector containing murine MyoD cDNA driven by the Rous sarcoma virus LTR [8]. This vector at a dose of 1000 or 200 pfu/cell allowed MyoD gene expression in 80 or 60% of cultured rat cardiac fibroblasts and only 14 or 2% of cells showed morphological changes towards myotubes, respectively. However, even with such a high transduction efficiency, only a minor portion of the MyoD positive cells differentiated into the muscle phenotype, according to microscopy. Perhaps a higher level of MyoD expression per cell is necessary for phenotypic conversion. Either a high levels of transduction or expression efficiency of the gene is required in target cells to increase the amount of MyoD protein. However, since a higher titer of the adenoviral vector is cytotoxic, the vector dose could not be increased [26,27].

We explored the notion that expression of the transduced gene could be increased through higher transcriptional or translational enhancement. In this context, we used the CAG promoter, which could generate more mRNA from the MyoD gene and thus increase the amount of MyoD protein expressed in infected cells even at a lower vector dose. We

constructed the novel adenoviral vector, Ad.CAGMyoD, which contains murine MyoD cDNA under the control of the powerful recombinant CAG promoter [15]. Using the above system at an moi of 10 in. cultured skin fibroblasts, Western blotting, which is not highly sensitive, confirmed MyoD protein expression. At an moi of 50, over 80% of primary fibroblasts were converted into myotubes, as confirmed by microscopy. We used murine MyoD cDNA for this experiment, however, human MyoD cDNA might be more increased the ratio of myogenic conversion of human fibroblasts efficiently.

The myoblast cell line, RD, which was derived from a human rhabdomyosarcoma, contains a very low level of MyoD protein that is undetectable by Western blotting (Fig. 1A). This indicated that maintenance of the myogenic phenotype such as that of RD requires only a small amount of MyoD, whereas the re-differentiation of well-differentiated fibroblasts into myogenic cells requires a considerably higher level of MyoD expression.

MyoD expression mediated by Ad.CAGMyoD was detected from 2 to 4 days after infection, which in fact was compatible with the physiological MyoD expression time course in regenerating muscle [24]. Therefore, cytotoxic effects were not evident in these cells for 3 weeks, during which they expressed the muscle-specific constructive protein, full-length dystrophin.

Molecular studies of cytoskeletal proteins in muscle cells have recently revealed that genetic abnormalities in dystrophin associated protein complexes in the sarcolemma, such as dystrophin [20], sarcoglycans [28], and merosin [29], are responsible for some types of progressive muscular dystrophies. Although the genes responsible for these diseases have been discovered, genetic diagnosis is not always possible because of the complex nature of the regulation of gene expression. When abnormalities are located in non-coding regions such as the introns or in the regulatory regions of the genes [30–32], PCR (multiplex and others) and/or cDNA sequencing cannot yield a diagnosis. Using the procedures described here, we obtained diagnoses at the level of proteins such as DMD and BMD, even when diagnosis by means of multiplex PCR and/or Southern blotting was impossible. For example, when biopsied muscle tissue was extremely damaged and/or non-specific (secondary) disappearance of the protein responsive gene product was suspected, in vitro myogenesis with our technique allowed a diagnosis. Further experiments are underway to examine the applicability of our technique to genetic muscle diseases other than DMD/BMD, such as congenital muscle dystrophies. DMD/BMD can be diagnosed in utero using amniotic fluid cells only when some genetic information is available [33]. Even in the absence of such information, in vitro myogenesis presents one potential option for diagnosis.

In addition, because large numbers of fibroblasts can be cultured, our system using in vitro myogenesis opens up the possibility of a basic strategy for the in vitro cell/organ engineering treatment of muscle diseases.

In conclusion, Ad.CAGMyoD exhibits high transduction efficiency with high levels of MyoD expression. Therefore, it should be a promising practical vector that could be an excellent candidate for the genetic diagnosis of myogenic diseases.

Acknowledgements

We thank Dr Y. Nabeshima for the generous gift of murine MyoD cDNA. This study was supported in part by grants (0176) from the Ministry of Health and Welfare of Japan.

References

[1] Ikezawa M, Minami N, Takahashi Y, Goto Y, Miike T, Nonaka I. Dystrophin gene analysis on 130 patients with Duchenne muscular dystrophy with a special reference to muscle mRNA analysis. Brain Dev 1998;20:165–8.
[2] Wedel DJ. Malignant hyperthermia and neuromuscular disease. Neuromuscul Disord 1992;2:157–64.
[3] Kawamura J. Detection of mutation in dystrophin gene in Duchenne muscular dystrophy-multiplex PCR and southern blot analysis (in Japanese). Nippon Rinsho Jpn 1997;55:3126–30.
[4] Roest PA, Bakker E, Fallaux FJ, Verellen-Dumoulin C, Murry CE, den Dunnen JT. New possibilities for prenatal diagnosis of muscular dystrophies: forced myogenesis with an adenoviral MyoD-vector. Lancet 1999;353:727–8.
[5] Ishikawa Y, Ishikawa Y, Minami R. Forced myogenesis with a retroviral MyoD-vector in human fibroblasts and dystrophin expression (in Japanese). No To Hattatsu Tokyo 2003;25:426–8.
[6] Kimura S, Ito K, Miyagi T, Hiranuma T, Yoshioka K, Ozasa S, et al. A novel approach to identify Duchenne muscular dystrophy patients for aminoglycoside antibiotics therapy. Brain Dev 2005;27:400–5.
[7] Weintraub H, Tapscott SJ, Davis RL, Thayer MJ, Adam MA, Lassar AB, et al. Activation of muscle-specific genes in pigment, nerve, fat, liver, and fibroblast cell lines by forced expression of MyoD. Proc Natl Acad Sci USA 1989;86:5434–8.
[8] Murry CE, Kay MA, Bartosek T, Hauschka SD, Schwartz SM. Muscle differentiation during repair of myocardial necrosis in rats via gene transfer with MyoD. J Clin Invest 1996;98:2209–17.
[9] Lattanzi L, Salvatori G, Coletta M, Sonnino C, Cusella De Angelis MG, Gioglio L, et al. High efficiency myogenic conversion of human fibroblasts by adenoviral vector-mediated MyoD gene transfer. An alternative strategy for ex vivo gene therapy of primary myopathies. J Clin Invest 1998;101:2119–28.
[10] Sancho S, Mongini T, Tanji K, Tapscott SJ, Walker WF, Weintraub H, et al. Analysis of dystrophin expression after activation of myogenesis in amniocytes, chorionic-villus cells, and fibroblasts. A new method for diagnosing Duchenne's muscular dystrophy. N Engl J Med 1993;329:915–20.
[11] Olson EN, Klein WH. bHLH factors in muscle development: dead lines and commitments, what to leave in and what to leave out. Genes Dev 1994;8:1–8.
[12] Rudnicki MA, Jaenisch R. The MyoD family of transcription factors and skeletal myogenesis. Bioessays 1995;17:203–9.
[13] Lopez-Casillas F, Riquelme C, Perez-Kato Y, Ponce-Castaneda MV, Osses N, Esparza-Lopez J, et al. Betaglycan expression is transcriptionally up-regulated during skeletal muscle differentiation.

Cloning of murine betaglycan gene promoter and its modulation by MyoD, retinoic acid, and transforming growth factor-beta. J Biol Chem 2003;278:382–90.
[14] Lassar AB, Paterson BM, Weintraub H. Transfection of a DNA locus that mediates the conversion of 10T1/2 fibroblasts to myoblasts. Cell 1986;47:649–56.
[15] Yuasa K, Miyagoe Y, Yamamoto K, Nabeshima Y, Dickson G, Takeda S. Effective restoration of dystrophin-associated proteins in vivo by adenovirus-mediated transfer of truncated dystrophin cDNAs. Fed Eur Biochem Soc Lett 1998;425:329–36.
[16] Fujii I, Suzuki S, Igarashi T, Matsukura M, Miike T. Shimada Targeted and stable gene delivery into muscle cells by a two-step transfer system. Biochem Biophys Res Commun 2000;275: 931–5.
[17] Kanegae Y, Makimura M, Saito I. A simple and efficient method for purification of infectious recombinant adenovirus. Jpn J Med Sci Biol 1994;47:157–66.
[18] Weintraub H, Davis R, Tapscott S, Thayer M, Krause M, Benezra R, et al. The myoD gene family: nodal point during specification of the muscle cell lineage. Science 1991;251:761–6.
[19] Capetanaki Y, Milner DJ, Weitzer G. Desmin in muscle formation and maintenance: knockouts and consequences. Cell Struct Funct 1997; 22:103–16.
[20] Hoffman EP, Brown RH, Kunkel LM. Dystrophin: the protein product of the Duchenne muscular dystrophy locus. Biotechnology 1992;24: 457–66.
[21] Okabe M, Ikawa M, Kominami K, Nakanishi T, Nishimune Y. 'Green mice' as a source of ubiquitous green cells. Fed Eur Biochem Soc Lett 1997;407:313–9.
[22] Davis RL, Cheng PF, Lassar AB, Weintraub H. The MyoD DNA binding domain contains a recognition code for muscle-specific gene activation. Cell 1990;60:733–46.
[23] Marshall P, Chartrand N, Worton RG. The mouse dystrophin enhancer is regulated by MyoD, E-box-binding factors, and by the serum response factor. J Biol Chem 2001;276:20719–26.
[24] Halevy O, Novitch BG, Spicer DB, Skapek SX, Rhee J, Hannon GJ, et al. Correlation of terminal cell cycle arrest of skeletal muscle with induction of p21 by MyoD. Science 1995;267:1018–21.
[25] Nonaka I. Pathophysiology in muscle fiber necrosis and regeneration with a particular reference to regenerating process (in Japanese). Rinsho Shinkeigaku Clin Neurol 1998;38:997–1000.
[26] Morral N, O'Neal W, Zhou H, Langston C, Beaudet A. Immune responses to reporter proteins and high viral dose limit duration of expression with adenoviral vectors: comparison of E2a wild type and E2a deleted vectors. Hum Gene Ther 1997;8:1275–86.
[27] Yang L, Lochmuller H, Luo J, Massie B, Nalbantoglu J, Karpati G, et al. Adenovirus-mediated dystrophin minigene transfer improves muscle strength in adult dystrophic (MDX) mice. Gene Ther 1998;5: 369–79.
[28] Holt KH, Campbell KP. Assembly of the sarcoglycan complex. Insights for muscular dystrophy. J Biol Chem 1998;273: 34667–70.
[29] Jones KJ, Kim SS, North KN. Abnormalities of dystrophin, the sarcoglycans, and laminin alpha2 in the muscular dystrophies. J Med Genet 1998;35:379–86.
[30] Kekou K, Florentin L, Metaxotou C. 3′ Acceptor splice site mutation in intron 50 leads to mild Duchenne muscular dystrophy phenotype. Hum Mutat 1998;1(Suppl.):S209–S12.
[31] Kimura S, Fujishita S, Ikezawa M, Ogawa M, Abe K, Miike T. Muscle type promoter and its first intron abnormalities in dystrophin gene in patients with Duchenne muscular dystrophy. J Child Neurol 1998;13: 290–2.
[32] Ikezawa M, Nishino I, Goto Y, Miike T, Nonaka I. Newly recognized exons induced by a splicing abnormality from an intronic mutation of the Dystrophin gene resulting in Duchenne muscular dystrophy. Hum Mutat 1999;13:170.
[33] Sancho S, Mongini T, Tanji K, Tapscott SJ, Walker WF, Weintraub H, et al. Analysis of dystrophin expression after activation of myogenesis in amniocytes, chorionic-villus cells, and fibroblasts. A new method for diagnosing Duchenne's muscular dystrophy. N Engl J Med 1993;329:915–20.

AAV1 Mediated Co-expression of Formylglycine-Generating Enzyme and Arylsulfatase A Efficiently Corrects Sulfatide Storage in a Mouse Model of Metachromatic Leukodystrophy

Toshiyuki Kurai[1], Sanae Hisayasu[1], Ryo Kitagawa[1], Makoto Migita[1], Hidenori Suzuki[2], Yukihiko Hirai[1] and Takashi Shimada[1]

[1]*Department of Biochemistry and Molecular Biology, Nippon Medical School, Bunkyo-ku, Tokyo, Japan;* [2]*Department of Pharmacology, Nippon Medical School, Bunkyo-ku, Tokyo, Japan*

Metachromatic leukodystrophy (MLD) is a lysosomal storage disorder caused by a deficiency of arylsulfatase A (ASA) and is characterized by deposition of sulfatide in all organs, particularly the nervous system. Recently, formylglycine-generating enzyme (FGE) was found to be essential for activation of sulfatases. This study examined the utility of FGE co-expression in AAV type 1 vector (AAV1)-mediated gene therapy of ASA knockout (MLD) mice. AAV1-ASA alone or AAV1-ASA and AAV1-FGE were co-injected into a single site of the hippocampus. Enzyme assay and immunohistochemical analysis showed that ASA was detected not only in the injected hemisphere but also in the non-injected hemisphere by 7 months after injection. Level of ASA activity and extent of ASA distribution were significantly enhanced by co-introduction of AAV1-FGE. Marked reductions in sulfatide levels were observed throughout the entire brain. The unexpectedly widespread distribution of ASA may be due to a combination of diffusion in extracellular spaces, transport through axons, and circulation in cerebrospinal fluid. The rotarod test revealed improvement of neurological functions. These results demonstrate that direct injection of AAV1 vectors expressing ASA and FGE represents a highly promising approach with significant implications for the development of clinical protocols for MLD gene therapy.

Received 5 January 2006; accepted 11 September 2006.
doi:10.1038/sj.mt.6300012

INTRODUCTION

Metachromatic leukodystrophy (MLD) is an autosomal recessive lysosomal disease caused by a deficiency of arylsulfatase A (ASA). MLD is characterized by accumulation of sulfatide and demyelination in the central and peripheral nervous systems causing severe progressive central nervous system symptoms.[1] Allogenic bone marrow transplantation in very early stages has been shown to be effective to delay disease progression in some cases,[2] but no specific treatment is currently available for the most frequent and severe late-infantile form of MLD. Like other lysosomal enzymes, part of ASA is excreted into the extracellular space and taken up by neighboring cells via a cation-independent mannose-6-phosphate receptor-mediated pathway.[3,4] This phenomenon, called cross-correction, is the rationale for enzyme replacement and gene therapy of lysosomal storage disorders without neurological lesions.[5–7] However, since the major target organ of MLD treatment is the nervous system, which is tightly guarded by the blood–brain barrier, the clinical efficacy of classical enzyme replacement therapy is likely to be limited.[8]

A possible method to treat neurological lesions is direct injection of viral vector carrying ASA in the brain. However, the major obstacle of this approach is how to distribute secreted ASA to the entire area of the large human brain. Even if the enzyme can cross correct surrounding non-transduced cells, multiple injections of large numbers of vector particles seem likely to be required if the whole brain is to be treated. Enhancement of gene expression may be important to minimize such invasive procedures.

Recent reports noted that post-translational formylation of a cysteine residue at the active site by formylglycine-generating enzyme (FGE) or sulfatase-modifying factors (SUMF1) is required for activation of all sulfatases, including ASA.[9–13] We have recently demonstrated that co-expression of FGE is essential for efficient expression and secretion of the active form of ASA in both cultured cells and mouse liver using plasmid vectors expressing ASA and FGE.[14] In cultured cells, FGE expression synergistically increased ASA activity up to 20-fold in cell lysates, and 70-fold in medium, indicating that the level of FGE is rate limiting.

ASA knockout mice have been extensively characterized[15–18] and are widely used as a mouse model for MLD.[4,19,20] The storage pattern of sulfatide is comparable to that of affected

Correspondence: Takashi Shimada, Department of Biochemistry and Molecular Biology, Nippon Medical School, 1-1-5 Sendagi, Bunkyo-ku, Tokyo 113-8602, Japan. E-mail: tshimada@nms.ac.jp

humans, but the degree of demyelination and neuromotor dysfunctions are mild and the mice have normal life span. ASA knockout mice have been recently treated by gene therapy approaches. Expression of ASA alone by lentiviral vector[19] and AAV vector[20] resulted in reduction of sulfatide storage and prevention of neuromotor impairment, suggesting that newly synthesized ASA was activated, at least partially, by endogenous FGE. However, it is not known whether endogenous FGE is sufficient for overexpression of active ASA in the brain. In the present study, we generated AAV1 vectors carrying ASA or FGE and examined the utility of FGE co-expression in AAV1-mediated direct gene therapy of MLD model mice.

RESULTS

Distribution of ASA in the brain

We generated three AAV serotype 1-based vectors expressing ASA and GFP (AAV1-ASA), FGE and GFP (AAV1-FGE), and GFP and neoR (AAV1-GFP). AAV1-ASA with or without AAV1-FGE was injected into the CA3 region of 8-month-old ASA-knockout mice (MLD mice). At 7 months after vector injection, ASA activity and enzyme distribution in the brain were examined using *p*-nitrocatechol sulfate and immunohistochemical methods, respectively. The brain was separated into three parts: the left (uninjected) hemisphere, the right (injected) hemisphere, and the cerebellum. Colorimetric enzyme assay with the artificial substrate *p*-nitrocatechol sulfate is known to reveal considerable background activities in ASA-null mice, probably due to nonspecific sulfatase activities.[21] However, a significant increase in sulfatase activity was detected in the injected hemisphere of MLD mice treated with AAV1-ASA. In addition, slightly increased sulfatase activities were seen in the uninjected hemisphere and cerebellum. Co-injection of AAV1-FGE significantly increased sulfatase activity throughout the entire brain, indicating a strong synergistic increase in ASA activity (**Figure 1a**).

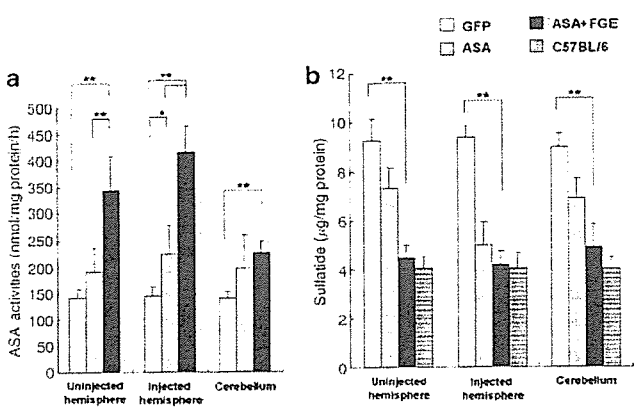

Figure 1 ASA activity and sulfatide content in the brain after direct AAV1 injection. The CA3 regions of the hippocampus of 8-month-old MLD mice were injected with AAV1 vectors and examined 7 months later. (**a**) ASA activity and (**b**) sulfatide content in the injected (ipsilateral) and uninjected (contralateral) hemispheres and cerebellum of MLD mice injected with AAV1-GFP ($n=6$), AAV1-ASA ($n=6$), and AAV1-ASA + AAV1-FGE ($n=7$) and age-matched C57BL/6 mice ($n=6$). Data represent mean + SEM. $^{*}P<0.01$; $^{**}P<0.001$.

Distribution pattern of ASA activity was studied by immunohistochemical analysis (**Figure 2**). Stereotactic injection of AAV1-GFP into the CA3 region of MLD mice resulted in strong GFP expression in cells around the injected area. In addition, GFP signals were seen throughout the hippocampus even on the non-injected side (**Figure 2a**), indicating efficient axonal transport of intracellular GFP molecules to the contralateral hemisphere. When AAV1-ASA and AAV1-FGE were coinjected, ASA-positive cells were clearly detected in pyramidal cell layers of the hippocampus on both injected and uninjected sides (**Figure 2d**). The distribution pattern of ASA is different from that of GFP. GFP positive cells were detectable only in the injected area, although GFP signals, not cell bodies, were seen within the whole hippocampal formation on both sides (**Figure 2c**). These results suggest that both ASA and GFP molecules are transported in the hippocampal commissure from cell bodies on the injected side to axon terminals on the uninjected side. ASA is excreted and recaptured by surrounding cells in both hemispheres, while GFP stays inside the cell bodies and axons.

The immunohistochemistry using the sensitive avidin–biotin–peroxidase complex method revealed that ASA was distributed in the whole brain including the fimbria, striatum, cerebral cortex, and cerebellum (**Figure 2e**). Punctuated staining in neurons and astrocytes revealed localization of ASA in lysosomes (**Figure 2e**, insets). To determine the phenotype of ASA expressing cells, immunohistochemical staining with cell-specific antibodies was performed. Most ASA positive cells were neurons. In addition, significant numbers of cells were labeled for ASA and GFAP, which is a marker of astrocytes. A few cells double labeled for ASA and IbaI, a microglia marker, were also detected, but we could not find ASA positive cells expressing GalC, a marker of oligodendrocytes. (**Figure 2f**).

Sulfatide content in the brain

Sulfatide storage in the brain of treated mice was analyzed by quantitative TLC analysis of lipid extracts and histochemistry (**Figures 1b** and **3**). MLD mice at 15 months old showed large amounts of accumulated sulfatide throughout the whole brain. Direct injection of AAV1-ASA at 8 months of age resulted in significant prevention of sulfatide storage in the injected hemisphere and moderate correction in the uninjected hemisphere and cerebellum. Remarkably, co-injection of AAV1-ASA and AAV1-FGE cleared accumulated sulfatide to the level of age-matched C57BL/6 mice in all brain areas (**Figure 1b**).

Prevention of sulfatide storage by AAV vector-mediated gene therapy was also demonstrated by Alcian blue staining (**Figure 3**). In MLD mice treated using control AAV1-GFP, Alcian blue-stained sulfatide was mainly detected in the hippocampal fimbria, internal capsules, and corpus callosum, as reported previously.[16] Alcianphilic granules were found in morphologically heterogeneous cells including large phagocyte and neuron like cells [4,16] (**Figure 3a**, inset). Injection of AAV1-ASA alone into the hippocampus CA3 region prevented accumulation of sulfatide on the injected side, but not on the uninjected side (**Figure 3b**). Co-injection of AAV1-ASA and AAV1-FGE resulted in total disappearance of deposits in all areas of the brain (**Figures 1b** and **3c**). In the cerebellum, sulfatide had

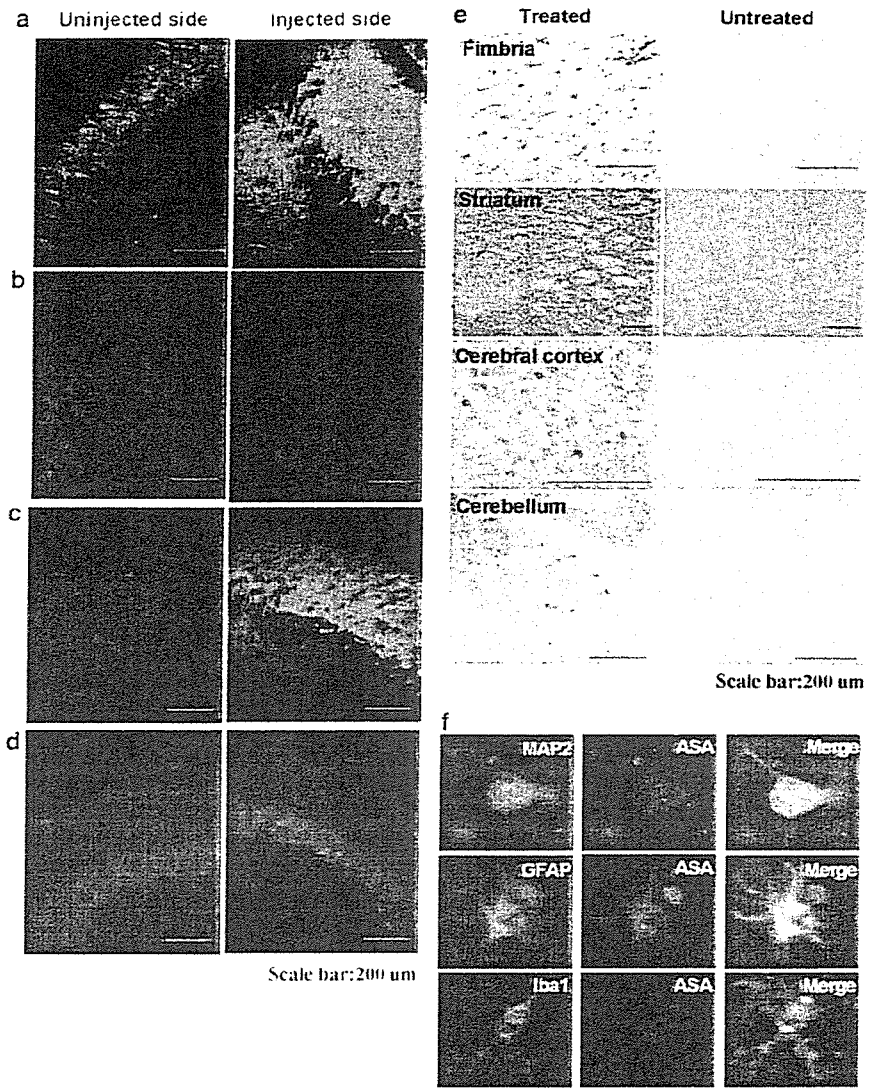

Figure 2 Distribution of ASA in the brains of MLD mice treated with AAV1 vectors. The CA3 regions of the hippocampus of 7-month-old MLD mice were injected with (**a**, **b**) AAV1-GFP or (**c**–**f**) AAV1-ASA and examined 5 months later. AAV1-ASA carries GFP cDNA as the second gene. Slices of the hippocampal regions were analyzed for (**a**, **c**) GFP expression or (**b**, **d**) ASA expression by immunostaining with anti-ASA antibody. ASA-positive cells were detected in both injected and uninjected sides, while GFP positive cells were mainly detected in the injected side. (**e**) Widespread expression of ASA was confirmed by DAB staining. Punctuated staining suggested localization of ASA in lysosomes (insets in **e**). (**f**) ASA positive cells were double-stained with antibodies for neurons (MAP2) astrocytes (GFAP) and microglia (Iba1).

predominantly accumulated in the white matter in untreated MLD mice, but was efficiently removed in mice treated using AAV1-ASA and AAV1 FGE (**Figure 3c**).

Neurological function

To evaluate neuromotor coordination and balance, MLD mice were analyzed by rotarod experiments. In the constant speed rotarod test of 15-month-old mice, untreated MLD mice exhibited highly impaired behavior compared to control C57BL/6 mice. The ASA-treated group showed better performance than the untreated group, but even more significant recovery was observed in the ASA + FGE treated group (**Figure 4a**). In the accelerating rotarod, no difference was observed between non-treated and treated MLD mice at the age of 12 months. However, behavioral deficit of untreated MLD mice became significant 3 months later. Injection of either AAV1-ASA alone or AAV1-ASA plus AAV1-FGE protected the progression of neurological impairment (**Figure 4b**).

DISCUSSION

FGE is localized in the endoplasmic reticulum and generates formylglycine from a cysteine residue at the active site of all sulfatases, including ASA. This post-translation modification occurs before folding of newly synthesized sulfatases[11,12] at luminal components of the endoplasmic reticulum.[13] Simultaneous co-expression of FGE and ASA in the same cell is thus essential and FGE activity represents a rate-limiting factor for generating the active form of ASA. Levels of human endogenous

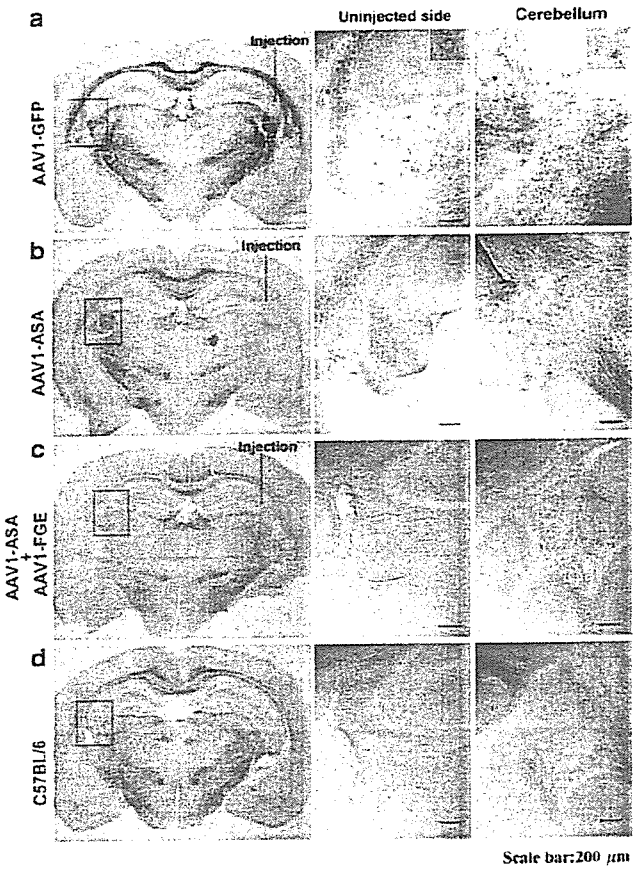

Figure 3 Correction of sulfatide storage in the brain after AAV1 vector injection. Deposits of sulfatide were identified by Alcian blue staining. Coronal sections of the brain and cerebellum from MLD mice injected with (**a**) AAV1-GFP (**b**) AAV1-ASA or (**c**) AAV1-ASA + AAV1-FGE and (**d**) from control C57BL/6 mice. In the mock-treated mouse, Alcian blue positive granules were seen in many cells including large phagocyte and neuron like cells (indicated by arrows and arrowheads, respectively, in the insets). (**c**) Sulfatide deposits on the uninjected side and the cerebellum were significantly reduced only after injection of AAV1-ASA + AAV1-FGE.

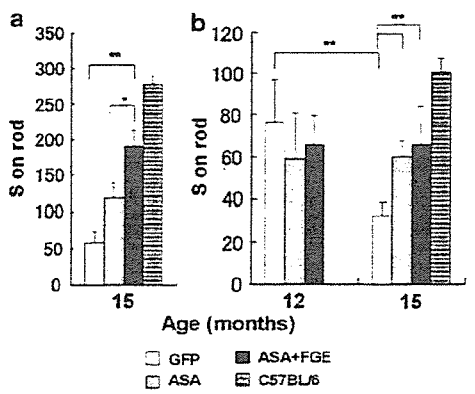

Figure 4 Rotarod performance of MLD mice. Eight-month-old MLD mice were treated with AAV1 vectors and neuromotor coordination and balance were analyzed by (**a**) the constant speed rotarod test at 15 months old or (**b**) the accelerating rotarod test at the age of 12 and 15 months. MLD mice injected with AAV1-GFP ($n = 10$), AAV1-ASA ($n = 9$), AAV1-ASA + AAV1-FGE ($n = 10$). Age-matched C57BL/6 mice ($n = 5$). Data represent mean + SEM. $^{*}P < 0.05$; $^{**}P < 0.01$.

FGE are reportedly high in the kidney and liver, but very low in the brain, suggesting that FGE co-expression should be required for overexpression of ASA in the human brain.[10,14] In contrast, expression of endogenous FGE in the mouse brain is moderate.[14] Indeed, previous studies have shown that direct injection of ASA expression vector alone into the mouse brain results in significantly increased ASA activity and phenotypic improvement.[19,20] Our data revealed, however, that FGE co-expression could further increase ASA activity in the mouse brain, suggesting that levels of endogenous FGE are insufficient for activation of overexpressed ASA. We have also found that ASA activity in the mouse liver was significantly increased by FGE co-expression, although endogenous FGE activity is relatively high (data not shown). We believe that co-expression of FGE with ASA should be considered for all types of MLD gene therapy.

Sevin *et al.*[20] recently reported successful gene therapy for MLD using AAV5 vector. In that study, multiple injection of AAV5 vector expressing ASA alone in the brain of MLD mice resulted in widespread distribution of ASA, reduction of sulfatide storage, and prevention of neuropathological abnormalities and neuromotor impairment. The present work demonstrated that similar therapeutic results can be obtained by co-injection of AAV1-ASA and AAV1-FGE at a single site. Although direct comparison of these two studies is difficult, AAV1 and AAV5 vectors appear equally useful for gene therapy against lysosomal disease targeting the central nervous system. However, irrespective of which vector system is used, co-expression of ASA and FGE appears to offer both theoretical and practical advantages over expression of ASA alone.

The finding that single vector injection was sufficient for prevention of sulfatide storage in the entire brain was somewhat surprising. This indicates that distribution of secreted ASA is unexpectedly efficient in the brain. Sustained secretion of large amounts of active ASA from brain cells achieved by co-injection of AAV1-ASA and AAV1-FGE would be a major contributor to this. In addition, other mechanisms may facilitate the widespread distribution of ASA. Axonal transport plays an important role in distant transfer of protein in the neuronal cells.[22,23] Our data clearly showed that anterograde transport of ASA (from cell bodies to axon terminals) is highly efficient and secreted ASA from axonal terminals on the contralateral side could be efficiently taken up by neighboring neuronal cell bodies.

Another possible route for distant transfer of ASA is through the cerebrospinal fluid. Although we did not intend intrathecal injection, it is possible that secreted ASA in the cerebrospinal fluid is distributed through the cerebrospinal fluid circulation to the entire central nervous system. Intrathecal administration of AAV2 vector carrying IDUA has recently been reported to result in widespread distribution in the brain, particularly in the cerebellum.[24]

In conclusion, this study offers the first demonstration of the utility of FGE co-expression in direct gene therapy for MLD model mice. AAV1-mediated expression of ASA and FGE resulted in long-term overexpression and secretion of functional ASA in the brain. Since levels of endogenous FGE are very low in the human brain, this strategy may have significant implications for the development of clinical protocols for MLD gene therapy.

MATERIALS AND METHODS

Plasmid construction and vector production. The plasmid pBEH/HT14-CP8 containing human ASA cDNA (X52151) was kindly donated by V Gieselmann. A clone (AK075459) containing full-length FGE cDNA sequence was purchased from the National Institute of Technology and Evaluation (Tokyo, Japan). The basic AAV vector plasmid was pAAV. CAαGBE plasmid, a derivative of psub201[25] and contained α-galactosidase A cDNA driven by the CAG promoter[26] as the first gene and GFP cDNA driven by the B19 promoter as the second gene.[6] The *Eco*RI fragment of the α-galactosidase cDNA of pAAV. CAαGBE was replaced by the *Eco*RI fragment of the ASA and FGE cDNAs. The resultant plasmids were named pAAV.CAhASABE and pAAV.CAhFGEBE, respectively. The AAV vector plasmid contained the GFP gene driven by the CAG promoter as the first gene and the neoR gene driven by the HSV-tymidine kinase promoter, pCAETKN, was used for generation of control GFP expression vector.

Recombinant AAV serotype 1 vector was generated by transfection using an adenovirus-free triple transfection method.[27] Briefly, the AAV vector plasmid, the *packaging* plasmid (p5E18RXC1; a gift from J Wilson)[28] and a helper plasmid (pHelper; Stratagene, La Jolla, CA) were co-transfected into HEK293 cells at a ratio of 1:1:1 under calcium phosphate precipitation. After 6 h of transfection, medium was replaced by fresh culture medium and cells were incubated for 50–60 h at 37°C under 5% CO_2. Cells were dislodged from culture dishes and pelleted by centrifugation, then resuspended in phosphate-buffered saline, freeze–thawed three times. Cell debris was spun down at 3,000 r.p.m. for 20 min at 4°C. AAV vectors were purified by ammonium sulfate precipitation and Iodixanol continuous gradient centrifugation[29] and ultrafiltrated using Centriprep YM10 concentrators (Millipore, Bedford, MA). Recombinant AAV1 vectors derived from pAAV.CAhASABE, pAAV.CAhFGEBE, and pCAETKN were named AAV1-ASA, AAV1-FGE, and AAV1-GFP, respectively. Genome titers of AAV vector were determined by slot-blot hybridization with the cDNA probe. Titer of the final preparation for each AAV vector was approximately 1.5×10^{12} vector genomes/ml.

Mouse model of MLD. ASA knockout mice were obtained from the laboratory of V. Gieselmann.[15] These mice have been extensively characterized and are widely used as a mouse model for MLD.[4,16,19,20,30] All animal experiments were performed in accordance with the regulations of the Ethics Committee of Nippon Medical School. For vector injection, mice were anesthetized using pentobarbiturate (10 mg/kg) and ketamine hydrochloride (6 mg/kg), then placed in a stereotactic frame. Skin over the skull was incised. The injection site was 2 mm posterior and 1.8 mm lateral to the bregma, and 2 mm dorsoventral from the skull surface. Approximately 7.5×10^9 particles of recombinant AAV vectors were delivered over a period of 5 min using a Hamilton syringe with a 33-G blunt-tip needle (Hamilton, Reno, NV).

Assay of arylsulfatase enzyme activity. The brain was cut into three sections (right and left hemispheres and cerebellum) and homogenized in pure water. Homogenates were centrifuged at 8,000 r.p.m. for 10 min at 4°C. ASA activity was measured using 10 mM *p*-nitrocatechol sulfate (Sigma, St Louis, MO) in a buffer consisting of 0.5 M sodium acetate (pH 5.0), 0.5 mM sodium pyrophosphate, and 10% sodium chloride.[14]

Histology. Mice were deeply anesthetized and perfused with phosphate-buffered saline followed by 4% paraformaldehyde. Brains were dissected and postfixed overnight at 4°C in 4% paraformaldehyde, and immersed in phosphate-buffered saline containing 30% sucrose. Brain sections were placed in OCT compound (Tissue-Tek; Sakura Finetechnical, Tokyo, Japan). Tissue sections were cut to a thickness of 20 μm and mounted on glass slides. Alcian blue staining was then performed to detect sulfatides.[31] Immunostaining for ASA protein was performed using anti-ASA rabbit IgG[14] and secondary anti-rabbit antibodies combined to Texas Red. ASA protein was also visualized by the avidin/biotinylated enzyme complex method using peroxidase and diaminobenzidine, according to the company's protocol (Vector Laboratories, Burlingame, CA).

To identify cell types, following antibodies were used: rabbit anti-MAP2 for neurons (Chemicon, Temecula, CA), anti-GFAP for astrocytes (Santa Cruz Biotechnology, Santa Cruz, CA), anti-Iba1 for microglias (Santa Cruz Biotechnology), and anti-GalC for oligodendrocytes (Sigma, St Louis, MO).

Quantification of sulfatide levels. Crude lipids were extracted from tissue homogenates as described by Folch *et al.*[32] Briefly, lipids were successively extracted with mixtures of chloroform/methanol (2/1, vol/vol), chloroform/methanol (1/1, vol/vol), and chloroform/methanol/water (86/14/1, vol/vol/vol). Glycosphingolipids recovered in Folch's lower phase were dried under a stream of nitrogen and then treated with mild alkaline (0.1 M NaOH in methanol) at 40°C for 1 h. After neutralizing the solution with 1 M acetic acid, glycosphingolipids were again recovered in Folch's lower phase and then applied to precoated high-performance thin-layer chromatography-silica gel 60F254 plates ($100 \times 200\ mm^2$, Art. 13728; E Merck, Darmstadt, Germany). The developing solvent used was chloroform/methanol/water (70/30/4, vol/vol/vol). After development, high-performance thin-layer chromatography plates were spread with 10% (w/v) cupric sulfate hydrate in 8% (v/v) phosphoric acid solution, then charred at 180°C for 10 min. Amounts were quantitatively determined by densitometric scanning using an AE6920M-CX image saver (Atto, Tokyo, Japan). Standard sulfatide was obtained from Wako Pure Chemical Industries (Osaka, Japan).

Rotarod test. Neuromotor coordination and balance were assessed by rotarod test using RRAC-3002 (O'Hara, Tokyo, Japan). In the constant speed rotarod test, mice were placed on the rotating rod at a constant speed of 6 r.p.m. and the duration for which an animal was able to stay on the rod was measured up to a maximum of 5 min. In the accelerating rotarod test, mice were placed on the rod at a speed of 4 r.p.m. Rotational speed gradually increased from 4 to 40 r.p.m. over 120 s and the latency to fall off were measured. Mice received four trials on the same day and their averages were presented.

Statistical analysis. Data from *in vivo* and *in vitro* experiments are expressed as mean ± SD. Differences between groups were tested for statistical significance using Student's *t*-test. An error level of 5% ($P < 0.05$) was considered significant.

ACKNOWLEDGMENTS

We thank V Gieselmann for providing ASA cDNA and ASA-knockout mice, K Ozawa for providing HEK293 cells and for discussion on the AAV production system, and M Yamamoto, M Nagano, and Y Ikeda for technical assistance and advice. This work was supported in part by grants from the Ministry of Health, Labor and Welfare of Japan and by the Ministry of Education, Science, and Culture of Japan.

REFERENCES

1. von Figura, K, Gieselmann, V and Jaeken, J (2001). Metachromatic leukodystrophy. *The Metabolic and Molecular Bases of Inherited Disease*. McGraw-Hill: New York, 8th edn. pp. 3694–3724.
2. Krivit, W (2004). Allogeneic stem cell transplantation for the treatment of lysosomal and peroxisomal metabolic diseases. *Springer Semin Immunopathol* **26**: 119–132.
3. Hille-Rehfeld, A (1995). Mannose 6-phosphate receptors in sorting and transport of lysosomal enzymes. *Biochim Biophys Acta* **1241**: 177–194.
4. Matzner, U *et al.* (2005). Enzyme replacement improves nervous system pathology and function in a mouse model for metachromatic leukodystrophy. *Hum Mol Genet* **14**: 1139–1152.

5. Sands, MS and Davidson, BL (2006). Gene therapy for lysosomal storage diseases. *Mol Ther* **13**: 839–849.
6. Takahashi, H *et al.* (2002). Long-term systemic therapy of Fabry disease in a knockout mouse by adeno-associated virus-mediated muscle-directed gene transfer. *Proc Natl Acad Sci USA* **99**: 13777–13782.
7. Sun, B *et al.* (2005). Correction of glycogen storage disease type II by an adeno-associated virus vector containing a muscle-specific promoter. *Mol Ther* **11**: 889–898.
8. Brady, RO and Schiffmann, R (2004). Enzyme-replacement therapy for metabolic storage disorders. *Lancet Neurol* **3**: 752–756.
9. Cosma, MP *et al.* (2003). The multiple sulfatase deficiency gene encodes an essential and limiting factor for the activity of sulfatases. *Cell* **113**: 445–456.
10. Dierks, T *et al.* (2003). Multiple sulfatase deficiency is caused by mutations in the gene encoding the human C(alpha)-formylglycine generating enzyme. *Cell* **113**: 435–444.
11. Dierks, T, Schmidt, B and von Figura, K (1997). Conversion of cysteine to formylglycine: a protein modification in the endoplasmic reticulum. *Proc Natl Acad Sci USA* **94**: 11963–11968.
12. Dierks, T, Miech, C, Hummerjohann, J, Schmidt, B, Kertesz, MA and von Figura, K (1998). Posttranslational formation of formylglycine in prokaryotic sulfatases by modification of either cysteine or serine. *J Biol Chem* **273**: 25560–25564.
13. Fey, J, Balleininger, M, Borissenko, LV, Schmidt, B, von Figura, K and Dierks, T (2001). Characterization of posttranslational formylglycine formation by luminal components of the endoplasmic reticulum. *J Biol Chem* **276**: 47021–47028.
14. Takakusaki, Y, Hisayasu, S, Hirai, Y and Shimada, T (2005). Coexpression of formylglycine-generating enzyme is essential for synthesis and secretion of functional arylsulfatase A in a mouse model of metachromatic leukodystrophy. *Hum Gene Ther* **16**: 929–936.
15. Hess, B *et al.* (1996). Phenotype of arylsulfatase A-deficient mice: relationship to human metachromatic leukodystrophy. *Proc Natl Acad Sci USA* **93**: 14821–14826.
16. Wittke, D, Hartmann, D, Gieselmann, V and Lullmann-Rauch, R (2004). Lysosomal sulfatide storage in the brain of arylsulfatase A-deficient mice: cellular alterations and topographic distribution. *Acta Neuropathol (Berl)* **108**: 261–271.
17. D'Hooge, R, Van Dam, D, Franck, F, Gieselmann, V and De Deyn, PP (2001). Hyperactivity, neuromotor defects, and impaired learning and memory in a mouse model for metachromatic leukodystrophy. *Brain Res* **907**: 35–43.
18. Schott, I, Hartmann, D, Gieselmann, V and Lullmann-Rauch, R (2001). Sulfatide storage in visceral organs of arylsulfatase A-deficient mice. *Virchows Arch* **439**: 90–96.
19. Consiglio, A *et al.* (2001). *In vivo* gene therapy of metachromatic leukodystrophy by lentiviral vectors: correction of neuropathology and protection against learning impairments in affected mice. *Nat Med* **7**: 310–316.
20. Sevin, C *et al.* (2006). Intracerebral adeno-associated virus-mediated gene transfer in rapidly progressive forms of metachromatic leukodystrophy. *Hum Mol Genet* **15**: 53–64.
21. Matzner, U, Harzer, K, Learish, RD, Barranger, JA and Gieselmann, V (2000). Long-term expression and transfer of arylsulfatase A into brain of arylsulfatase A-deficient mice transplanted with bone marrow expressing the arylsulfatase A cDNA from a retroviral vector. *Gene Therapy* **7**: 1250–1257.
22. Luca, T *et al.* (2005). Axons mediate the distribution of arylsulfatase A within the mouse hippocampus upon gene delivery. *Mol Ther* **12**: 669–679.
23. Passini, MA, Lee, EB, Heuer, GG and Wolfe, JH (2002). Distribution of a lysosomal enzyme in the adult brain by axonal transport and by cells of the rostral migratory stream. *J Neurosci* **22**: 6437–6446.
24. Watson, G *et al.* (2006). Intrathecal administration of AAV vectors for the treatment of lysosomal storage in the brains of MPS I mice. *Gene Therapy* **13**: 917–925.
25. Samulski, RJ, Chang, LS and Shenk, T (1987). A recombinant plasmid from which an infectious adeno-associated virus genome can be excised *in vitro* and its use to study viral replication. *J Virol* **61**: 3096–3101.
26. Miyazaki, J *et al.* (1989). Expression vector system based on the chicken beta-actin promoter directs efficient production of interleukin-5. *Gene* **79**: 269–277.
27. Salvetti, A *et al.* (1998). Factors influencing recombinant adeno-associated virus production. *Hum Gene Ther* **9**: 695–706.
28. Gao, GP, Alvira, MR, Wang, L, Calcedo, R, Johnston, J and Wilson, JM (2002). Novel adeno-associated viruses from rhesus monkeys as vectors for human gene therapy. *Proc Natl Acad Sci USA* **99**: 11854–11859.
29. Hermens, WT *et al.* (1999). Purification of recombinant adeno-associated virus by iodixanol gradient ultracentrifugation allows rapid and reproducible preparation of vector stocks for gene transfer in the nervous system. *Hum Gene Ther* **10**: 1885–1891.
30. D'Hooge, R, Coenen, R, Gieselmann, V, Lullmann-Rauch, R and De Deyn, PP (1999). Decline in brainstem auditory-evoked potentials coincides with loss of spiral ganglion cells in arylsulfatase A-deficient mice. *Brain Res* **847**: 352–356.
31. Scott, JE and Dorling, J (1965). Differential staining of acid glycosaminoglycans (mucopolysaccharides) by alcian blue in salt solutions. *Histochemie* **5**: 221–233.
32. Folch, J, Lees, M and Sloane-Stanley, GH (1957). A simple method for the isoloation and purification of total lipids from animal tissues. *J Biol Chem* **226**: 497–509.

Neuroscience 144 (2007) 743–753

NEURONAL SPECIFICITY OF α-SYNUCLEIN TOXICITY AND EFFECT OF PARKIN CO-EXPRESSION IN PRIMATES

T. YASUDA,[a] S. MIYACHI,[b] R. KITAGAWA,[c] K. WADA,[d] T. NIHIRA,[d] Y.-R. REN,[d] Y. HIRAI,[c] N. AGEYAMA,[e] K. TERAO,[e] T. SHIMADA,[c] M. TAKADA,[b] Y. MIZUNO[a,d] AND H. MOCHIZUKI[a,d]*

[a]*Research Institute for Diseases of Old Ages, Juntendo University School of Medicine, Bunkyo-ku, Tokyo 113-8421, Japan*

[b]*Tokyo Metropolitan Institute for Neuroscience, Tokyo Metropolitan Organization for Medical Research, Fuchu, Tokyo 183-8526, Japan*

[c]*Department of Biochemistry and Molecular Biology, Nippon Medical School, Bunkyo-ku, Tokyo 113-8602, Japan*

[d]*Department of Neurology, Juntendo University School of Medicine, Bunkyo-ku, Tokyo 113-8421, Japan*

[e]*Tsukuba Primate Research Center, National Institute of Biomedical Innovation, Tsukuba, Ibaraki 305-0843, Japan*

Abstract—Recombinant adeno-associated viral (rAAV) vector-mediated overexpression of α-synuclein (αSyn) protein has been shown to cause neurodegeneration of the nigrostriatal dopaminergic pathway in rodents and primates. Using serotype-2 rAAV vectors, we recently reported the protective effect of Parkin on αSyn-induced nigral dopaminergic neurodegeneration in a rat model. Here we investigated the neuronal specificity of αSyn toxicity and the effect of Parkin co-expression in a primate model. We used another serotype (type-1) of AAV vector that was confirmed to deliver genes of interest anterogradely and retrogradely to neurons in rats. The serotype-1 rAAV (rAAV1) carrying *αSyn* cDNA (rAAV1-αSyn), and a cocktail of rAAV1-αSyn and rAAV1 carrying *parkin* cDNA (rAAV1-parkin) were unilaterally injected into the striatum of macaque monkeys, resulting in protein expression in striatonigral GABAergic and nigrostriatal dopaminergic neurons. Injection of rAAV1-αSyn alone decreased tyrosine hydroxylase immunoreactivity in the striatum compared with the contralateral side injected with a cocktail of rAAV1-αSyn and rAAV1-parkin. Immunostaining of striatonigral GABAergic neurons was similar on both sides. Overexpression of Parkin in GABAergic neurons was associated with less accumulation of αSyn protein and/or phosphorylation at Ser129 residue. Our results suggest that the toxicity of accumulated αSyn is not induced in non-dopaminergic neurons and that the αSyn-ablating effect of Parkin is exerted in virtually all neurons in primates.

*Correspondence to: H. Mochizuki, Department of Neurology, Juntendo University School of Medicine, Bunkyo-ku, Tokyo 113-8421, Japan. Tel: +81-3-3813-3111; fax: +81-3-3814-3016.
E-mail address: hideki@med.juntendo.ac.jp (H. Mochizuki).

Abbreviations: DARPP-32, dopamine- and cAMP-regulated phosphoprotein of 32 kDa; DAT, dopamine transporter; EGFP, enhanced green fluorescent protein; PB, phosphate buffer; PBS, phosphate-buffered saline; PD, Parkinson's disease; rAAV, recombinant adeno-associated virus; SNpc, substantia nigra pars compacta; SNpr, substantia nigra pars reticulata; αSyn, α-synuclein; TH, tyrosine hydroxylase; VMAT2, vesicular monoamine transporter 2.

Key words: Parkinson's disease, adeno-associated virus, dopaminergic neurons, GABAergic neurons, monkey.

Parkinson's disease (PD) is a progressive neurodegenerative disorder affecting approximately 1% of people over the age of 65 (Goedert, 2001). The disease is clinically characterized by akinesia, rigidity, resting tremor, and postural instability. The pathological hallmarks of PD are the selective loss of dopaminergic neurons in the substantia nigra pars compacta (SNpc), and the presence of eosinophilic protein inclusions termed Lewy bodies in the surviving SNpc dopaminergic neurons. Based on the finding that a point mutation in the gene encoding α-synuclein (αSyn) protein causes a rare familial form of PD (PARK1) (Polymeropoulos et al., 1997; Kruger et al., 1998; Zarranz et al., 2004), αSyn has been confirmed to be a major component of Lewy bodies in patients with sporadic PD (Spillantini et al., 1997). Abnormal accumulation of αSyn protein has widely been hypothesized as a neurotoxic event in PD development (Goedert, 2001). Recent studies indicated that another dominantly inherited form of familial PD, PARK4, is caused by triplication of the *αSyn* gene locus (Singleton et al., 2003). This genetic mutation results in production of higher levels of αSyn protein, supporting the αSyn-induced neurodegeneration hypothesis. However, in cell types other than the dopaminergic one, the overexpressed αSyn protein sometimes functions as a neuroprotective molecule (da Costa et al., 2000; Xu et al., 2002). Thus, oxidative modification of αSyn by dopamine metabolites is considered responsible for the selective vulnerability to dopaminergic neurons (Conway et al., 2001; Xu et al., 2002). Based on the above studies, clearance of abnormal αSyn protein from SNpc dopaminergic neurons can be potentially used as a strategy in the treatment of PD.

The viral vector-mediated αSyn delivery causes accumulation of αSyn and subsequent degeneration of SNpc dopaminergic neurons in adult rodents and primates (Kirik et al., 2002, 2003; Klein et al., 2002; Lo Bianco et al., 2002; Lauwers et al., 2003; Yamada et al., 2004). Using a recombinant adeno-associated viral (rAAV) vector, we previously showed that αSyn protein that accumulated in rat SNpc dopaminergic neurons is phosphorylated at serine residue of 129th position (Ser129) (Yamada et al., 2004). In fact, such post-translational modification is frequently observed in human brains affected with so-called α-synucleinopathy, including PD and dementia with Lewy bodies (Fujiwara et al., 2002). Recent studies also showed that Ser129-phosphorylation of αSyn is essential for neurodegeneration in a *Drosophila* model of PD (Chen and Feany, 2005).

0306-4522/07$30.00+0.00
doi:10.1016/j.neuroscience.2006.09.052

The major cause of autosomal recessive juvenile Parkinsonism (ARJP) is a mutation in the gene encoding Parkin protein (PARK2) (Kitada et al., 1998). Parkin is an E3 ubiquitin ligase that catalyzes polyubiquitination of unfolded or short-lived proteins, directing the substrates to proteasomal degradation (Shimura et al., 2000). The PARK2 mutation results in loss-of-function of Parkin protein. It was reported recently that oxidative post-translational modifications of Parkin, e.g. *S*-nitrosylation (Chung et al., 2004; Yao et al., 2004) or covalent binding of dopamine (LaVoie et al., 2005), may be responsible for impairment of Parkin activity in sporadic cases of PD. Such processes could lead to accumulation of substrate proteins with subsequent dopaminergic neurodegeneration as proposed in PARK2 patients. We reported previously that rAAV-mediated overexpression of Parkin ameliorates the αSyn-induced SNpc dopaminergic neurodegeneration in a rat model (Yamada et al., 2005). Another group has shown similar results using a lentiviral vector (Lo Bianco et al., 2004). These data suggest that Parkin delivery may be therapeutically beneficial not only in PARK2 patients but also in patients with sporadic PD.

The aim of the present study was to assess the neuronal specificity of αSyn toxicity and the effect of Parkin delivery in a primate model with αSyn overexpression. While a serotype-2 rAAV vector was used in our previous studies (Yamada et al., 2004, 2005), here we applied another serotype (type-1) of rAAV (rAAV1) vector that could deliver genes of interest anterogradely and retrogradely to neurons. Injections of rAAV1 vectors producing enhanced green fluorescent protein (EGFP) (rAAV1-EGFP), αSyn (rAAV1-αSyn) and/or Parkin protein (rAAV1-parkin) into the rat and monkey striatum resulted in protein expression in striatonigral GABAergic and nigrostriatal dopaminergic neurons. Moreover, the overexpression of αSyn protein certainly decreased the density of dopaminergic axon terminals in the striatum, which was ameliorated by co-expression of Parkin protein.

EXPERIMENTAL PROCEDURES

Animals

Five adult male Sprague–Dawley rats (10-week-old) (Nihon SLC, Hamamatsu, Japan) were used for this study. The experimental protocol was approved by the Ethics Review Committee for Animal Experimentation of Juntendo University School of Medicine.

Two male crab-eating monkeys (*Macaca mullata*; 3.5–4.5 kg body weight) were used for this study. Intrastriatal injections of AAV vectors were carried out in a biosafety level-2 laboratory at the Tsukuba Primate Research Center which was designated for *in vivo* infectious experiments. The experimental protocol was approved by the Animal Care and Use Committee of the Tokyo Metropolitan Institute for Neuroscience and by the Animal Welfare and Animal Care Committee of the Tsukuba Primate Research Center. All experiments were conducted according to the U.S. National Institutes of Health Guide for the Care and Use of Laboratory Animals, the Guideline for the Care and Use of Animals (Tokyo Metropolitan Institute for Neuroscience 2000) and the Rules for Animal Care and Management of the Tsukuba Primate Research Center. Throughout the experiments, the best efforts were made to minimize the number of animals used and their suffering.

Generation of rAAV vectors

The plasmid DNA *pAAV-MCS* (CMV promoter; Stratagene, La Jolla, CA, USA) carrying human *αSyn* cDNA (pAAV-MCS-αSyn) was constructed as reported previously (Yamada et al., 2004). Human *parkin* or *EGFP* cDNA was cloned into plasmid pAAV-MCS (pAAV-MCS-parkin or pAAV-MCS-EGFP, respectively). The plasmid DNA pAAV-MCS-αSyn, pAAV-MCS-parkin, or pAAV-MCS-EGFP was co-transfected with plasmids pHelper and Pack2/1 to HEK293 cells using a standard calcium phosphate method (Sambrook and Russell, 2001). After 48 h, the cells were harvested and crude rAAV vector solutions were obtained by repeated freeze/thaw cycles. After ammonium sulfate precipitation, virus particles were dissolved in phosphate-buffered saline (PBS) and applied to an OptiSeal centrifugation tube (Beckman Coulter, Inc., Fullerton, CA, USA). After overlaying an OptiPrep solution (Axis-Shield PoC AS, Oslo, Norway), the tube was processed by GradientMaster (BioComp Instruments, Inc., Fredericton, NB, Canada) to prepare a gradient layer of OptiPrep. The tube was then ultracentrifuged at 13,000 r.p.m. for 18.5 h. The fractions containing high-titer rAAV vectors were collected and used for injection into animals. The number of rAAV genome copies was semi-quantified by PCR within the CMV promoter region using primers 5′-GACGTCAATAATGACGTATG-3′ and 5′-GGTAATAGCGATGACTAATACG-3′. The final titers were 6.4×10^{11} genomes/mL (rAAV1-EGFP), 5.5×10^{11} genomes/mL (rAAV1-αSyn), and 7.0×10^{12} genomes/mL (rAAV1-parkin).

Stereotaxic injection of rAAV vectors

The rats were anesthetized with sodium pentobarbital (40 mg/kg body weight, i.p.). They were positioned in a stereotaxic frame. The skull was exposed, and a small portion of the skull over the striatum was removed unilaterally with a dental drill. Subsequently, rAAV1-EGFP was injected into the striatum (3 μL; 1.92×10^9 particles, 0.5 mm anterior and 2.9 mm lateral from bregma, 6.5 mm below the dural surface, tooth bar=4.0 mm) through a 5-μL Hamilton microsyringe.

After a survival period of 3 weeks, the rats were anesthetized deeply with sodium pentobarbital (100 mg/kg, i.p.) and perfused transcardially with PBS, followed by 4% paraformaldehyde in PBS. The brains were removed from the skull, postfixed in the same fresh fixative overnight, and immersed in PBS containing 30% sucrose until they sank. Coronal sections were cut serially at 20 μm thickness by a freezing microtome.

The monkeys were first sedated with ketamine hydrochloride (5 mg/kg, i.m.) and xylazine hydrochloride (0.5 mg/kg, i.m.), and then anesthetized with sodium pentobarbital (20 mg/kg, i.v.). After bilateral removal of skull portions over the striatum, stereotaxic injections of rAAV1-αSyn were made unilaterally into the putamen, and those of a cocktail of rAAV1-αSyn and rAAV1-parkin were made contralaterally. A total of 50 μL of each vector preparation was injected at five rostrocaudally different levels (10 μL each) through a 50-μL Hamilton microsyringe (50 μL on the side injected with rAAV1-αSyn alone; 2.75×10^{10} particles, and 100 μL on the side co-injected with rAAV1-αSyn; 2.75×10^{10} particles, and rAAV1-parkin; 3.5×10^{11} particles).

After survival periods of 4 and 7.5 months, the monkeys were anesthetized deeply with sodium pentobarbital (50 mg/kg, i.p.) and perfused transcardially with PBS, followed by a mixture of 8% formalin and 15% saturated picric acid in 0.1 M phosphate buffer (PB; pH 7.4). The brains were removed from the skull, postfixed in the same fresh fixative overnight, and immersed in PB containing 30% sucrose until they sank. Coronal sections were cut serially at 60 μm thickness by a freezing microtome.

Antibodies and immunohistochemistry

The primary antibodies used in this study were as follows; rabbit anti-GFP (diluted at 1:200; Chemicon International Inc., Te-

mecula, CA, USA), mouse anti-αSyn (clone LB509; 1:100; Zymed Laboratories Inc., South San Francisco, CA, USA), mouse anti-Ser129-phosphorylated αSyn (clone pSyn#64; 1:10,000; Wako Pure Chemical Industries, Osaka, Japan), sheep anti-tyrosine hydroxylase (TH) (1:5000; Calbiochem, San Diego, CA, USA), rabbit anti-vesicular monoamine transporter 2 (VMAT2) (1:200; Chemicon International Inc.), rabbit anti-dopamine transporter (DAT) (1:200; Chemicon International Inc.), rabbit anti-Parkin (1:500; Cell Signaling Technology Inc., Beverly, MA, USA), rabbit anti-dopamine- and cAMP-regulated phosphoprotein of 32 kDa (DARPP-32) (1:100; Chemicon International Inc.), and rat anti-substance P (1:100; Chemicon International Inc.) antibodies. Every fourth 20-μm-thick (rats) and every tenth 60-μm-thick (monkeys) free-floating coronal section of brain was washed in PBS, soaked with 10% Block Ace (Yukijirushi-Nyugyo Co., Sapporo, Japan) in PBS, and then incubated at 4 °C for 24–48 h with primary antibody dissolved in a PBS medium containing 2% Block Ace and 0.05% Triton X-100. Subsequently, for colorimetric visualization of the antigen, the sections were incubated for 2 h in the same fresh medium containing biotinylated secondary antibody (anti-mouse, anti-rabbit, anti-rat, or anti-sheep IgG antibody; 1:500; Vector Laboratories Inc., Burlingame, CA, USA), followed by avidin–biotin–peroxidase complex (ABC Elite; Vector Laboratories Inc.) for another 1 h. Then the sections were reacted in 0.05 M Tris–HCl buffer (pH 7.6) containing 0.04% diaminobenzidine and 0.002% hydrogen peroxide with (dark brown/purple color) or without (brown color) 0.04% nickel chloride. Images were captured using a light microscope (ACT-1, Nikon Corporation, Tokyo, Japan). For fluorescent double or triple staining of the antigens, FITC-, Cy3-, or Cy5-conjugated anti-mouse, anti-rabbit, anti-rat, or anti-sheep IgG antibody (1:500; Jackson ImmunoResearch Laboratories, Inc., West Grove, PA, USA) was used as secondary antibody. Fluorescent images were captured using a fluorescent microscope (AxioVision, Zeiss, Jena, Germany) or a confocal laser-scanning microscope (LSM510, Zeiss).

Densitometric quantification, cell counting, and statistical analysis

The densities of TH-, VMAT2-, DAT- or substance P-positive fibers were quantified using the NIH Image software. Four different areas (0.5-mm×0.5-mm) randomly selected from dorsolateral portion of the putamen (for TH, VMAT2 and DAT, shown by open ellipse in Fig. 4A, B) or from ventrolateral portion of the substantia nigra pars reticulata (SNpr; for substance P, shown by open ellipse in Fig. 4E, F) each from three different sections were used for densitometric quantification. For the TH-positive cell counting, every tenth coronal section including the whole SNpc area was used. Similarly, every tenth section including the whole putamen area was used for the αSyn-positive cell counting. Six randomly selected sections including the medial part of the putamen were used for counting the Ser129-phosphorylated αSyn-positive cells. To count the number of DARPP-32-positive cell bodies in the putamen, 12 different areas (0.2-mm×0.2-mm) adjacent to the track of the injection needle (shown by filled arrowheads in Fig. 4C, D) each from three different sections were randomly selected. Two-tailed Student's t-test was applied to evaluate a statistical significance between the groups. A P value <0.01 (**) and <0.001 (***) was denoted as a significant difference.

RESULTS

rAAV1 vector-mediated expression of EGFP protein in rat brain

We first generated a high-titer rAAV1 vector carrying *EGFP* cDNA (rAAV1-EGFP) and injected it stereotaxically into the rat striatum. Examination of the expression pattern of EGFP in the substantia nigra showed positive immunostaining of cell bodies and axon terminals in the SNpc and the SNpr, respectively (Fig. 1A–F). Confocal microscopy analysis revealed that the EGFP-positive cell bodies in the SNpc were also immunoreactive for TH (Fig. 1A–C inset, white arrowhead), and that the EGFP-positive axon terminals in the SNpr were immunoreactive for substance P (Fig. 1D–F). In the striatum, the expression of EGFP was noted in cell bodies immunoreactive for DARPP-32 (Fig. 1G–I, white arrowhead). These findings indicate that the injection of the rAAV1 vector into the striatum results in anterograde transport of the delivered gene along the striatonigral GABAergic pathway and in retrograde direction along the nigrostriatal dopaminergic pathway. Using this serotype of rAAV, we generated in the next step a primate model of PD induced by αSyn-mediated neurodegeneration, and examined the effect of co-expression of Parkin in the model.

rAAV1 vector-mediated overexpression of αSyn and Parkin proteins in monkey brain

High-titer rAAV1 vectors necessary to produce αSyn (rAAV1-αSyn) and Parkin (rAAV1-parkin) proteins were prepared. In two monkeys, rAAV1-αSyn alone was injected into the putamen area of the striatum on one side, while a cocktail of rAAV1-αSyn and rAAV1-parkin was injected on the opposite side. Following rAAV vector-mediated protein expression, the monkeys exhibited no obvious behavioral abnormalities. After 4- and 7.5-month post-injection period, the monkeys were killed and the expression patterns of αSyn and Parkin proteins were determined. In both monkeys, αSyn was noted in neuronal cell bodies in the putamen (Fig. 2C, D) and in axon terminals in the SNpr (data not shown). Immunohistochemical analysis using a monoclonal antibody that specifically recognizes the Ser129-phosphorylated αSyn protein (clone pSyn#64) revealed that the accumulated αSyn protein was subjected to post-translational Ser129-phosphorylation modification (Fig. 2E, F). The Ser129-phosphorylated αSyn proteins were co-localized with DARPP-32 in the putamen (Fig. 3A–C, white arrowhead) and with substance P in the SNpr (Fig. 3D–F). These results confirm the anterograde transport of the delivered gene along the striatonigral GABAergic pathway.

In the hemisphere injected with a cocktail of rAAV1-αSyn and rAAV1-parkin, a similar expression pattern of Parkin protein was observed in each monkey (Fig. 2B). Furthermore, we found co-expression of αSyn and Parkin proteins in SNpc dopaminergic neurons (Fig. 3G–J, white arrowhead). The number of these neurons was 25–30 cells/section in one monkey (killed at the 4-month post-injection period) and fewer than five cells/section in the other monkey (killed at the 7.5-month post-injection period). These results confirm the retrograde transport of the delivered gene along the nigrostriatal dopaminergic pathway. In each monkey, αSyn-positive dopaminergic cell bodies were only rarely detected on the side injected with rAAV1-αSyn alone (data not shown).

Effect of αSyn overexpression and co-expression of Parkin on nigrostriatal dopaminergic neurons

In the monkey killed at the 4-month post-injection period, striatal immunoreactivity for TH was lower in the putamen on

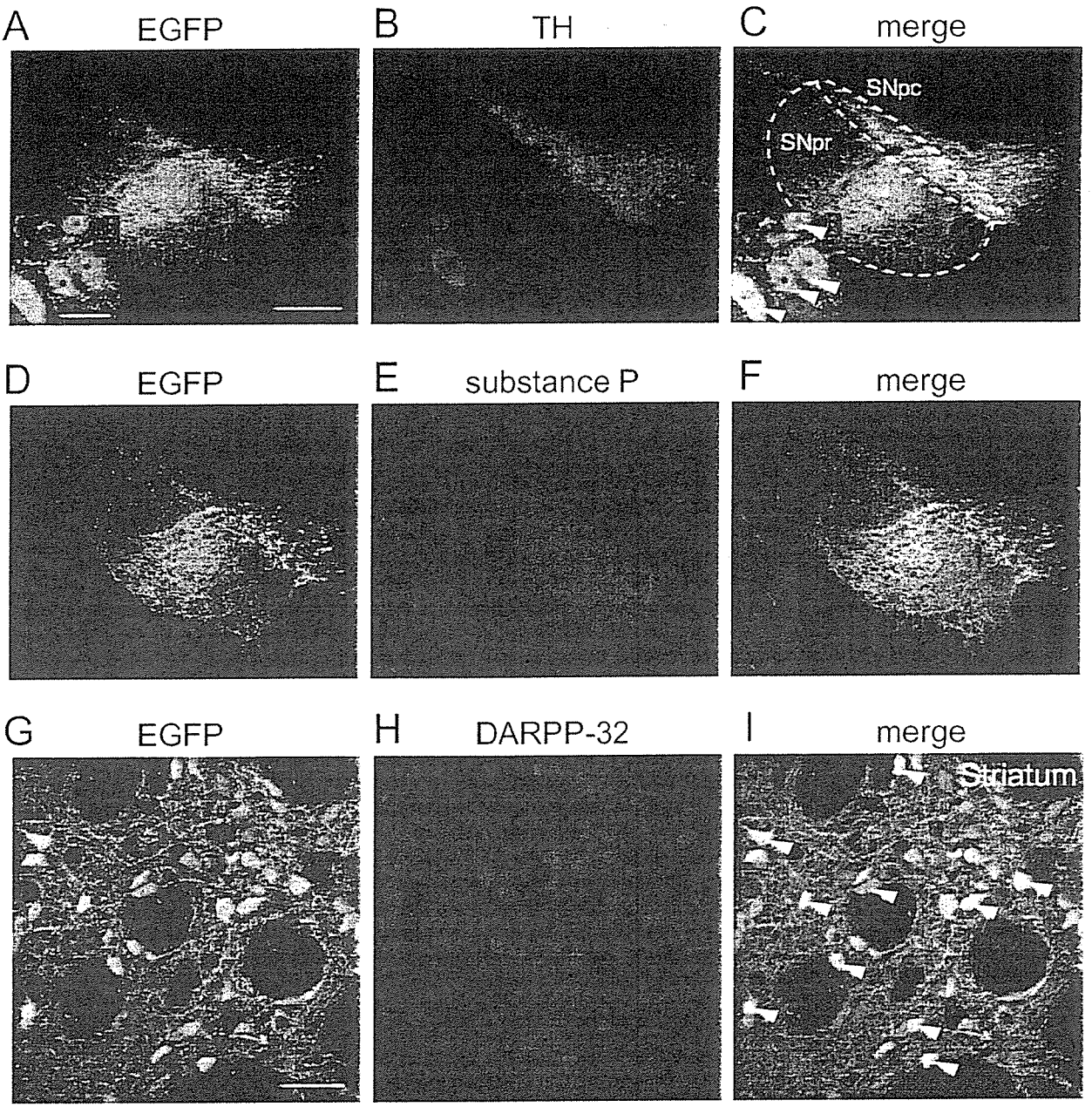

Fig. 1. rAAV1-mediated expression of EGFP protein in rat brain. Immunoreactivity for EGFP protein in the substantia nigra (SN) (A–F) and the striatum (G–I). (A–C) The EGFP-positive cell bodies (A) are immunoreactive with TH (B) in the SNpc (C), indicating gene delivery to dopaminergic neurons (A–C inset, white arrowheads: enlarged images captured by confocal microscopy). (D–I) The EGFP-positive axon terminals in the SNpr (D) are immunoreactive with substance P (E). Image analysis by confocal microscopy shows co-localization of the EGFP-positive cell bodies (G) with DARPP-32 (H) in the striatum (I, white arrowheads). These findings indicate gene delivery to GABAergic neurons. Scale bar = 400-μm in A (A–F); in A inset, 25-μm; and in G, 25-μm (G–I). The SNpc and the SNpr are circumscribed by dotted white lines in C.

the side injected with rAAV1-αSyn alone, compared with the side injected with a cocktail of rAAV1-αSyn and rAAV1-parkin (compare Fig. 4A and B inset). This was observed throughout the entire rostrocaudal extent of the putamen. We quantified the densities of the TH-positive axon terminals in the dorsolateral area of putamen (shown by open ellipse in Fig. 4A, B) and found a statistically significant difference between the two sides (Fig. 5A, TH+). Similar findings were noted with immunostaining for VMAT2 and DAT (Fig. 5A, VMAT2+ and DAT+). However, there was no significant change in the number of TH-positive cell bodies in the SNpc compared on each side (Fig. 5B, C). No differences in TH, VMAT2 and DAT immunoreactivities were noted in the monkey killed at the 7.5-month post-injection period.

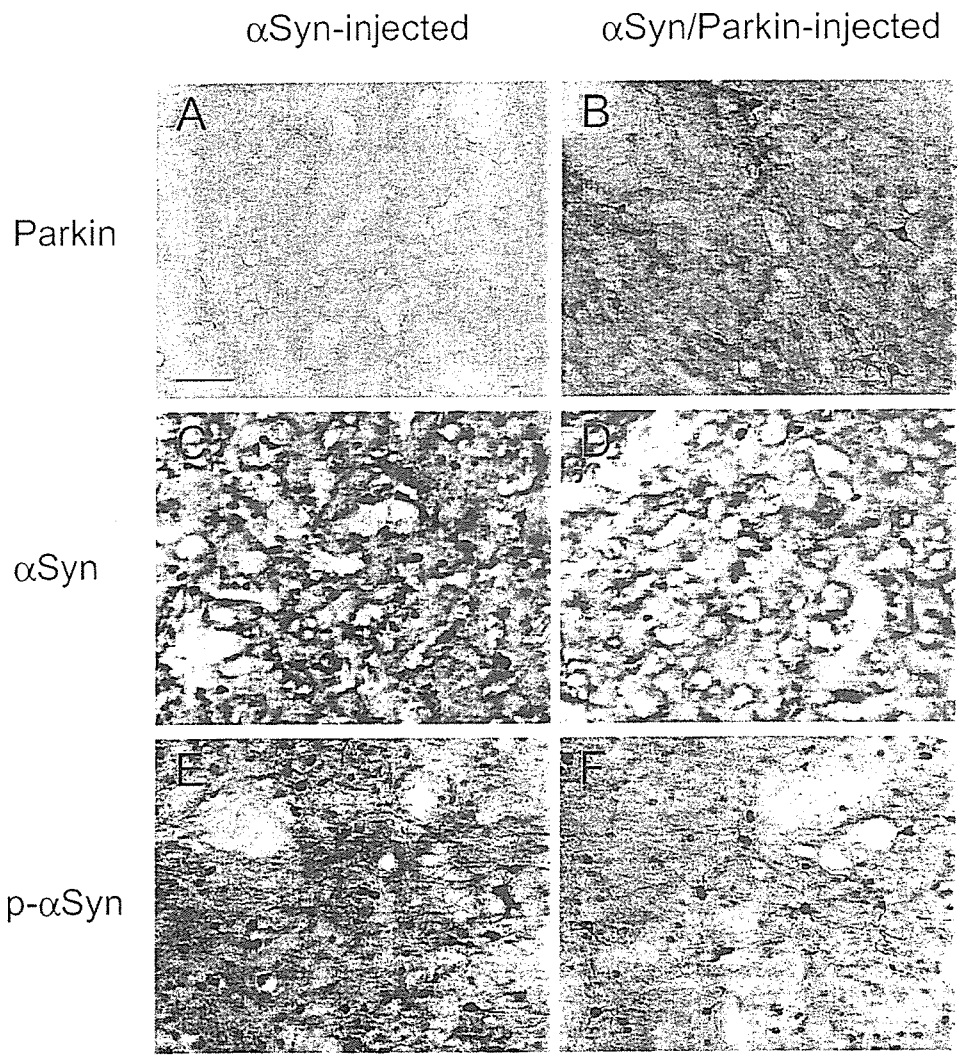

Fig. 2. Immunostaining for Parkin, αSyn, and Ser129-phosphorylated αSyn (p-αSyn) proteins in the monkey putamen. Photographs of the side injected with rAAV1-αSyn alone (A, C, and E; αSyn-injected) and the side injected with a cocktail of rAAV1-αSyn and rAAV1-parkin (B, D, and F; αSyn/Parkin-injected) are represented. The immunoreactivities for *Parkin* (A and B), *αSyn* (C and D), or p-αSyn (E and F) in the putamen are indicated. Note that accumulation and/or Ser129-phosphorylation of αSyn protein are less on the side injected with a cocktail of rAAV1-αSyn and rAAV1-parkin. Scale bar=50-μm in A (A–F).

Effect of αSyn overexpression and co-expression of Parkin on striatonigral GABAergic neurons

In both monkeys, we analyzed striatal immunoreactivity for DARPP-32 and nigral immunoreactivity for substance P. No apparent reduction of DARPP-32 and substance P immunoreactivity on the side injected with rAAV1-αSyn only was observed in comparison with the side co-injected with rAAV1-αSyn and rAAV1-parkin (Fig. 4C–F, and C, D inset). Quantification of the number of DARPP-32-positive cells in the putamen and the density of substance P-positive axon terminals in the SNpr showed no statistically significant differences between the two sides (Fig. 6A, B).

However, immunostaining of striatal and nigral sections with anti-αSyn and anti-Ser129-phosphorylated αSyn antibodies showed a lower degree of accumulation and/or Ser129-phosphorylation of αSyn protein on the Parkin-delivered side (compare Fig. 2C and D, and E and F). These results were consistent throughout the entire rostrocaudal extents of the putamen (Fig. 6C and D, αSyn; E and F, Ser129-phosphorylated αSyn) and SNpr. These results suggest that aberrantly accumulated αSyn does not induce neurotoxicity of GABAergic neurons and that the αSyn-ablating effect of the overexpressed Parkin is not only exerted on dopaminergic neurons but also on GABAergic neurons.

DISCUSSION

In the present study, we analyzed the neuronal specificity of αSyn toxicity and the effect of Parkin co-expression in primates. We applied the serotype-1 rAAV as a substitute for serotype-2 rAAV (rAAV2) that has been used in our previous studies (Yamada et al., 2004, 2005). We found

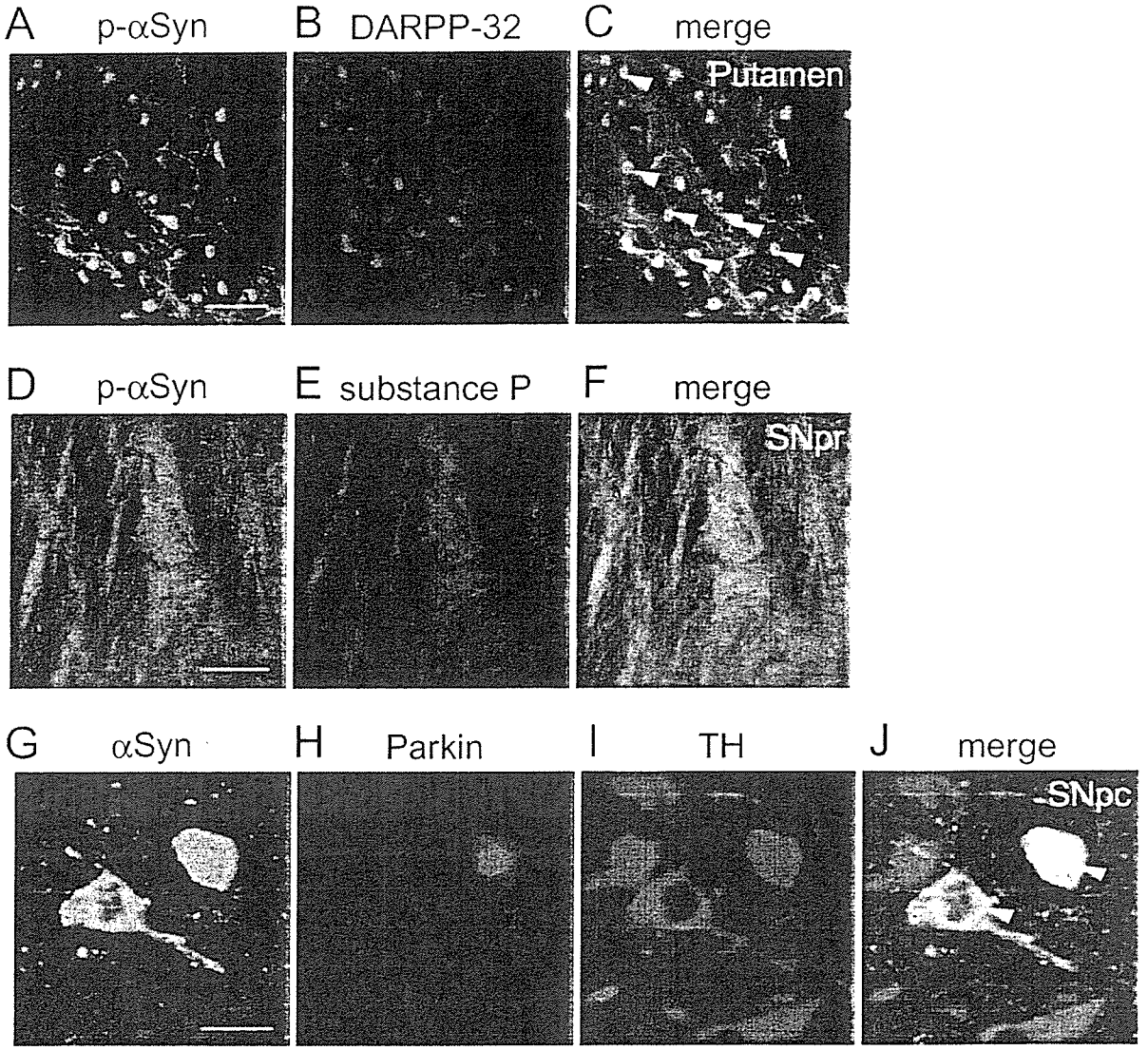

Fig. 3. Image analysis by confocal microscopy for αSyn, Ser129-phosphorylated αSyn (p-αSyn), and Parkin proteins expressed in monkey brain. (A–F) Overexpressed αSyn protein is phosphorylated at Ser129 residue in GABAergic neurons. (A–C) The p-αSyn-positive cells (A) are immunoreactive with DARPP-32 (B) in the putamen (C, white arrowheads). (D–F) The p-αSyn-positive axon terminals in the SNpr (D) are immunoreactive with substance P (E). (G–J) Co-expression of αSyn (G) and Parkin proteins (H) in TH-positive dopaminergic neurons (I) in the SNpc (J, white arrowheads). Scale bar = 100-μm in A (A–C); in D, 50-μm (D–F); and in G, 25-μm (G–J).

several advantages for rAAV1 application, including the reduction of time to prepare high-titer viral stocks and their ability to express transgenes more rapidly, compared with rAAV2 (data not shown). Furthermore, rAAV1 vectors did not only show anterograde but also retrograde transport of delivered genes. This property will be valuable when neuroprotective molecules including Parkin are supplied to SNpc dopaminergic neurons in human PD patients. In this regard, direct stereotaxic injections of viral vectors into the SNpc, which is situated deep in the brain, carries a high risk of surgical injury of other normal brain regions. In addition, viral injections into spatially larger striatal tissue can be performed with greater certainty.

αSyn transgenic mouse models of PD have been reported to exhibit abnormal accumulation of αSyn protein in neurons and to show abnormal behavioral phenotypes (Masliah et al., 2000; van der Putten et al., 2000; Matsuoka et al., 2001; Giasson et al., 2002; Lee et al., 2002; Neumann et al., 2002; Richfield et al., 2002; Rockenstein et al., 2002; Gispert et al., 2003; Hashimoto et al., 2003; Martin et al., 2006). **However, such models hardly display any pathology in the SNpc, especially the loss of dopaminergic neurons. By contrast, the viral vector-mediated αSyn delivery has been shown to cause αSyn accumulation in dopaminergic neurons in the SNpc and their subsequent degeneration** (Kirik et al., 2002, 2003; Klein et al., 2002; Lo Bianco et al., 2002; Lauwers et al., 2003; Yamada et al., 2004). **In at least one of the two monkeys examined in the present study, TH immunoreactivity was decreased in the striatum after injection of rAAV1-αSyn alone, as compared**